FILE

INTERNAL DOCUMENT

102

I.O.S.

STORM SURGE PREDICTIONS BY THE QUASI UNIFOR STEADY WIND/PRESSURE FIELD METHOD

(1)

S. Ishiguro

1981

[*This document should not be cited in a published bibliography, and is supplied for the use of the recipient only*].

NATURAL ENVIRONMENT RESEARCH COUNCIL

INSTITUTE OF OCEANOGRAPHIC SCIENCES

INSTITUTE OF OCEANOGRAPHIC SCIENCES

Wormley, Godalming,
Surrey GU8 5UB
(042-879-4141)

(Director: Dr. A. S. Laughton)

Bidston Observatory,
Birkenhead,
Merseyside L43 7RA
(051-653-8633)
(Assistant Director: Dr. D. E. Cartwright)

Crossway,
Taunton,
Somerset TA1 2DW
(0823-86211)
(Assistant Director: M. J. Tucker)

INSTITUTE OF OCEANOGRAPHIC SCIENCES

INTERNAL DOCUMENT 102

STORM SURGE PREDICTIONS BY THE QUASI UNIFORM STEADY WIND/PRESSURE FIELD METHOD

(1)

S. Ishiguro

1981

Institute of Oceanographic Sciences
Wormley, Surrey, England

CONTENTS

ABSTRACT

A new practical dynamic method for predictions of storm surges (positive and negative, coastal and offshore) in the North Sea has been developed with two variations: Type-A for daily-surges, and Type-B for an extreme surge occurring once in many (say 50) years.

The method has been based on the finding that a high surge in the sea is generated by a sustained wind/pressure field with an almost steady direction and a high wind speed. Such a field is represented by a simple field with a constant direction and magnitude over a finite duration. This is indicated by only three factors which characterize each storm case: wind direction, wind speed and duration. Factors for the pressure field are derived from the three factors.

A set of four water-level responses at each point in the North Sea is computed from the surge dynamic equations (or a model). Two of them are responses to two constant wind fields in orthogonal directions, and the other two are those for similar pressure fields. Each field is suddenly applied to the sea in a calm state. The responses are expressed in a generalized form for an arbitrary intensity of the fields.

Combining the above three factors and four responses by a simple additional computation, the maximum surge height at each point can be obtained for each specific surge case. Since the values of the responses are independent from each surge case, the set of responses can be used repeatedly.

For Type-A prediction, the three factors are obtained from forecast wind/pressure data. For Type-B prediction, only an extreme wind speed derived from a statistical analysis of observed wind data is available. Therefore, a technique to determine the maximum surge height at each point, only from the extreme wind speed, has been developed.

The simplified representation of a 'real' wind/pressure field by the three factors produces an error, other than errors associated with conventional dynamic surge computations. The error is reduced by the dynamic system of the sea which responds to an average value of external forces. Also the error tends to reduce when a surge is high, since a high surge is generated by an intense wind field which is closer to a simplified representation.

The above-mentioned simplification significantly benefits the practical surge prediction, particularly for Type-A: e.g. (1) surge data for the initial conditions of a dynamic computation is not required; (2) the very small amount of input data needed from a weather forecaster can be transmitted even by telephone; (3) a simple additional computation for each surge case can be carried out by a small computer in a short time; and (4) a minor running cost.

The method offers the prediction of the maximum surge height at each point in each surge case only, which the public is most interested in, and not the time-varying surge height.

The method has been tested with 17 surge cases, two of which are shown in this paper. A set of 44 surge cases which supports the method is also shown. The accuracy of the method is justified, compared with that of the weather forecast on which the overall accuracy of a surge prediction is based. Comparisons of the method with other methods, and plans for further improvements are also shown.

1. INTRODUCTION

The North Sea has a history of disastrous coastal floods due to storm surges. Heavy traffic in the sea, including large vessels, requires more critical information of water level which is related to daily surge predictions. The recent increase in offshore constructions, due to the exploration of the North Sea for oil, requires extreme surge values in the long term, as well as daily surges.

Several surge prediction methods have been developed for the North Sea, starting with empirical-formula methods. The development of dynamic-computation methods have made predictions of surges offshore possible which were previously difficult. The advance of the meteorological forecasting, particularly with the introduction of a large-scale computer, has brought a good prospect of surge predictions by a combined operation of meteorological and surge models. However, these methods have not yet been used for routine surge-prediction services. One of the weak points of dynamics methods is their complexity which involves a large amount of data being transmitted and computed, and therefore the facilities and running cost of a routine service becomes considerable.

The method described in this paper is a dynamic method, and preserves all beneficial parts of dynamic methods, such as a high capability of simulation of a surge phenomenon in a sea having a complex topography and dynamic conditions. A significant simplification of the method from the operational aspect is derived from (1) the simplification of its input wind/pressure data, and (2) the limitation of its output to the maximum surge height only (not the time-varying surge height). (1) is based on the finding that a high surge is generated by a wind/pressure field which is close to a uniform steady field. (2) satisfies most of the requirements of the public (the prediction of the timing of the occurrence of the maximum depends on the weather forecast).

The method has two variations, Type-A for daily-surge predictions, and Type-B for a long-term extreme surge prediction. Both variations are based on the same principle. Predicted values by Type-A procedure can be evaluated from observed values which are easily available. Information on the accuracy of Type-A prediction can be extended to that of Type-B, which cannot be evaluated by the observational values in a short period.

The method can be used with any other dynamic method, providing that it can produce a set of values of X, Y, J, K, as described in this paper. The author has obtained these values from one of his own electronic models (a dynamic model though not numerical). This paper contains the results using the values from his previous model, and another paper to be issued will contain the results using the values from his new electronic model. A part of the method, Type-B, was first applied in 1966. It has been expanded toward Type-A, and now with the two variations, is still being improved.

2. EXAMPLES OF QUASI UNIFORM STEADY WIND/PRESSURE FIELD

The North Sea is sometimes covered by a sustained wind field having an almost steady direction with a high wind speed. Generally, the wind direction in the whole sea area varies slightly following the curvature of isobars, and also varies slightly due to the movement of the weather system. The wind speed varies with area and time, to a greater degree than the wind direction. The author calls this state a quasi uniform steady wind/pressure field, and finds that a high storm surge in the sea is generated by such a field.

Each of 17 storm-surge cases in the North Sea have been examined from this point of view, only two examples being shown in this chapter. Also, 44 storm-surge cases have been examined as a set of data which supports this theory.

In order to make the investigation objective, observational data (with minimum computational processes) have been used. Since historical observational surge data are limited to coastal ones, surge heights observed at coastal stations only are investigated with quasi uniform steady wind/pressure fields found in weather maps.

2.1 Surge on 3rd January 1976

Fig. 1 shows the wind/pressure field and surge in the North Sea on 3rd January 1976, sampled at 3-hourly intervals. The wind/pressure field is based on observational data analysed by Harding & Binding (1978). The pressure field is shown by isobars (solid lines) with 2 mb intervals, and the wind field by equal-speed lines (dotted lines) with 10 kt intervals. The surge heights along the coast are shown by a bar graph*, taking surge height on the vertical axis, and the approximate position of each station on the horizontal axis with the abbreviation of the name of the station (see Appendix 1 for the full name and exact position).

When the depression centre is in the sea area (00 to 03 GMT), the surge heights are not great, with quite random polarities, since the surge is generated on a local scale by various wind directions in the sea area.

After the centre has moved out from the sea area (06 to 09 GMT), the wind direction in the sea area has become more uniform, although the speed varies with area and time. The development of a high positive surge can be seen along the Netherlands and German coasts which are leeward of the wind field. A negative surge can also be seen around the south Norwegian coast which is windward of the field.

Throughout the rest of the period (12 to 21 GMT), the wind field is still sustained with a minor change of direction and the gradual decay of its speed. The surge height along the Netherlands and German coasts starts to decay, while that around Southend increases (due to a slight change of the wind direction).

---

*This format of representation of surge heights is used throughout this paper, since it is convenient in this prediction model to see the surge heights along the coast at a sampled time.

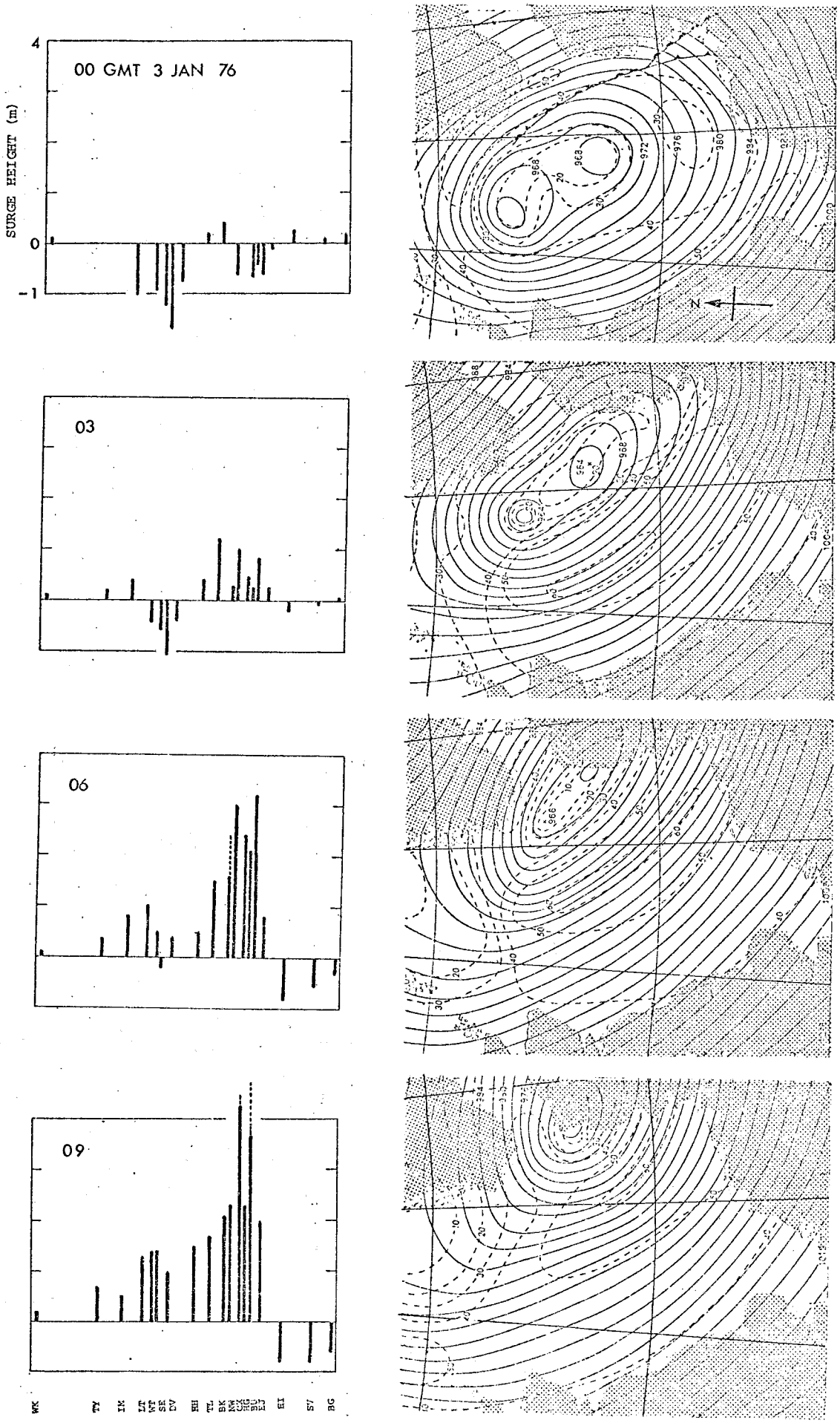

Fig. 1 Wind/pressure field and surge heights observed along the North Sea coast on 3rd January 1976.

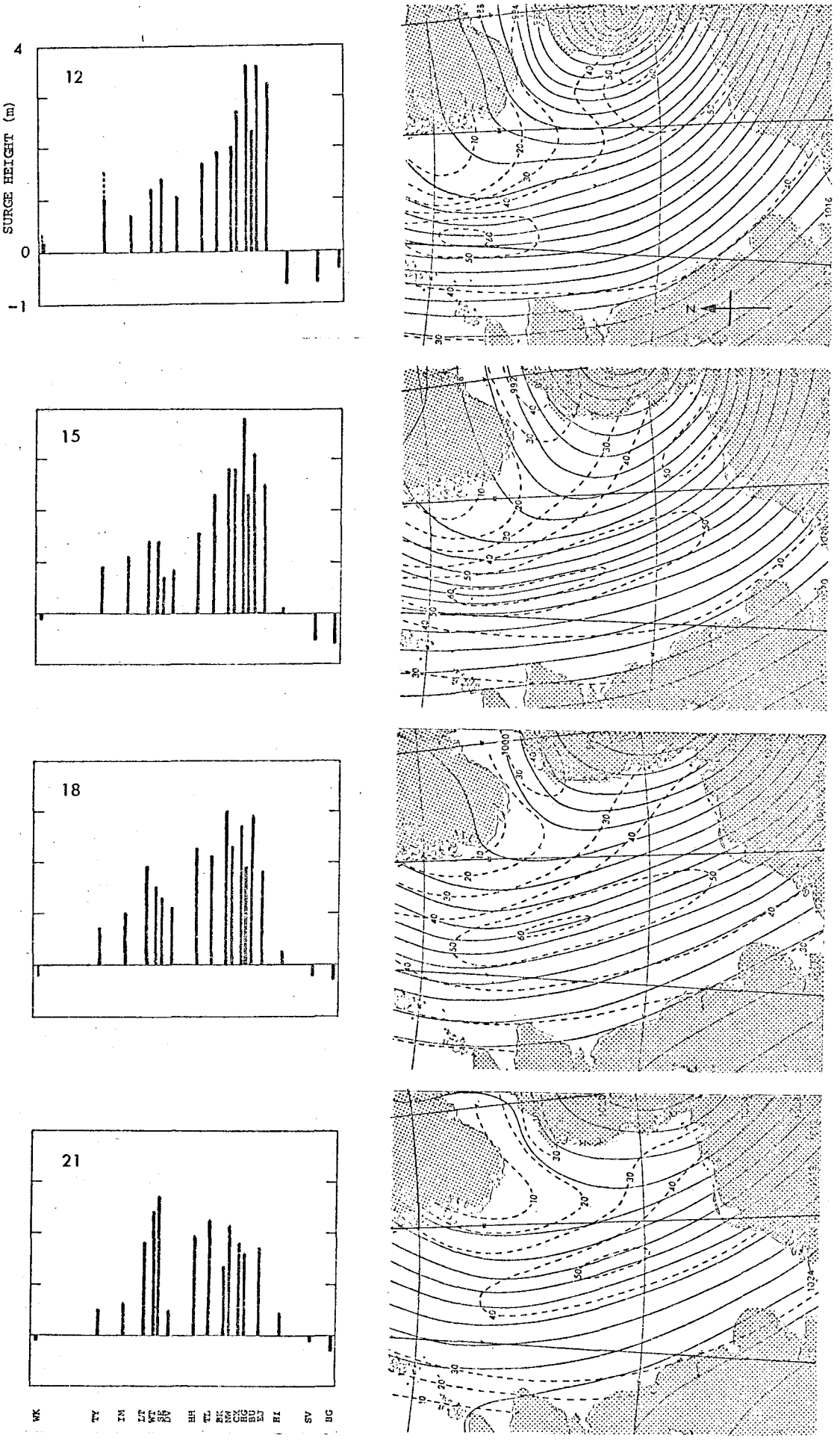

(Fig. 1 continued)

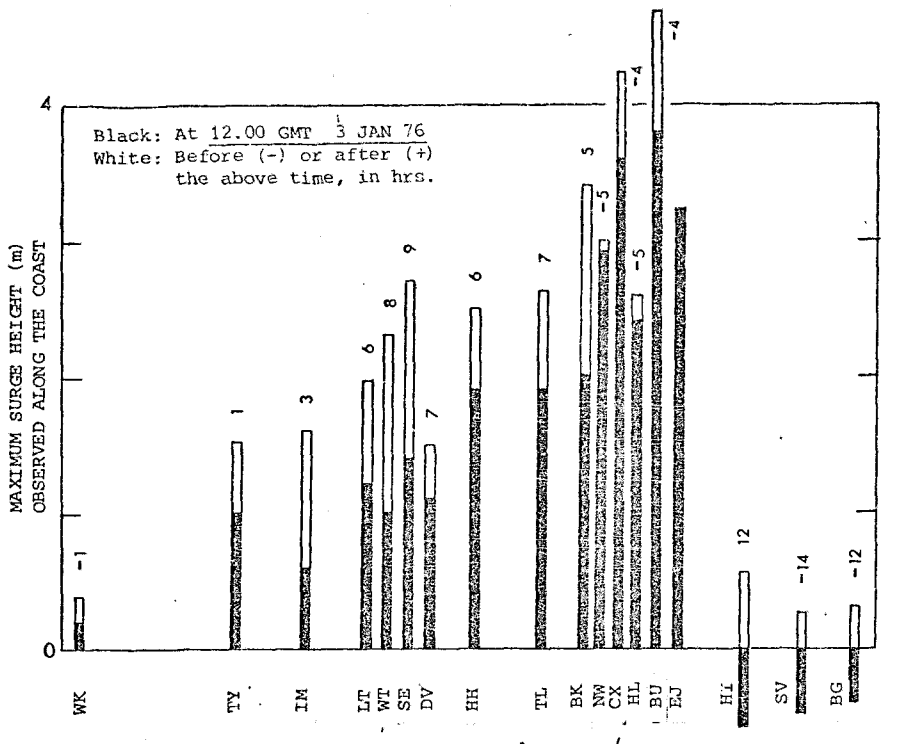

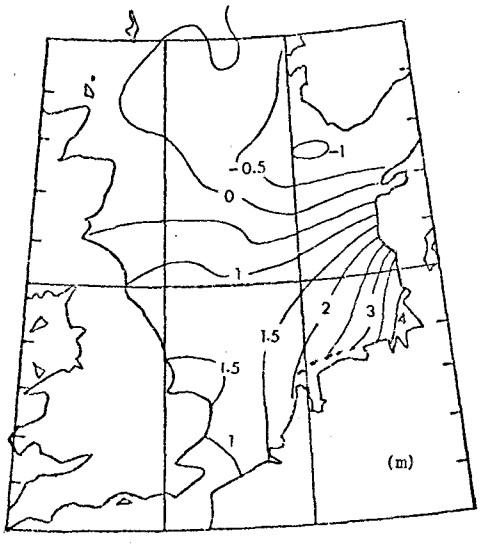

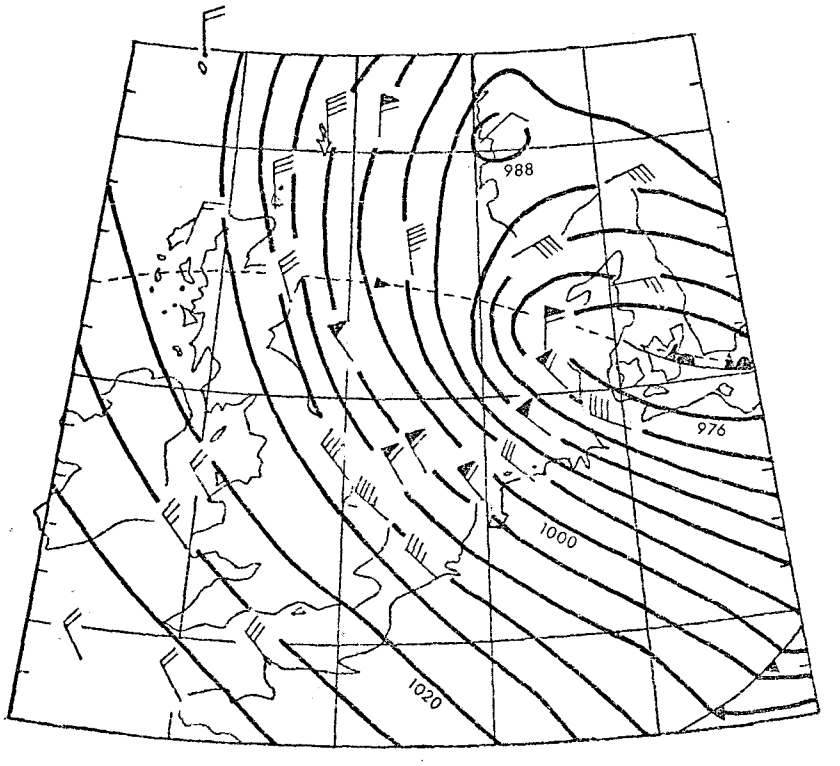

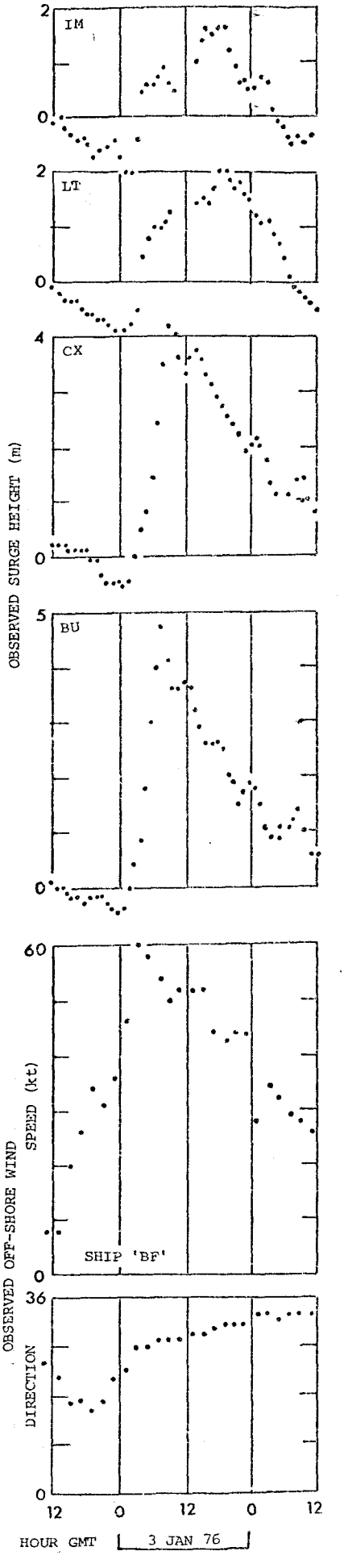

Fig. 2 Summary diagrams of the surge on 3rd January 1976.

Fig. 2 shows a set of diagrams which summarizes this surge case from the point of view of the formation of a quasi uniform steady wind/pressure field.

The bar graph shows the surge along the North Sea coast. The envelope of this graph shows the maximum surge height during this surge case. The black part of the bar shows the surge height at the sampled time.

Surge height variations with time observed at a few representative coastal stations are shown in the top-right of Fig. 2. Since the surge observed offshore is not available, this is represented by a computed contour map for the sampled time (obtained from another dynamic method) and is shown in the centre of Fig. 2.

The wind/pressure field is represented by a synoptic weather map for a time nearest to the sampled time. The variations of representative wind speed and direction observed at an offshore station are shown in the bottom-right of Fig. 2.

2.2 Surge on 1st February 1953

Fig. 3 is a similar diagram to Fig. 1, but for the surge around 1st February 1953. A set of diagrams to the left side of Fig. 3 shows the wind field on the sea surface. This wind field has been obtained from the observational data, by using the 'meteorological input-data processing system' (Ishiguro, 1979b). The pressure data is based on combined material supplied from the UK Meteorological Office and the Netherlands Meteorological Institute. The set of bar graphs to the right side of Fig. 3 shows the surge height along the North Sea coast. The data are based on Rossiter (1954) and the Netherlands Delta Committee (1960), and are combined by the author.

A similar relationship between the wind/pressure field and surge generation to the previous example can be seen in this surge case. Namely, when the depression centre is in the sea area (12 GMT, 31st January), the surge heights are not great and their polarity is quite random. After the centre has moved out from the sea area (15 GMT), the development of the surge starts. The direction of the wind field is very steady for about 24 hours. The distribution of the surge height along the coast, and their variation with time, clearly correspond to the direction of the wind field and the variation of wind speed with time, throughout the period. The surge is fully developed at 06 GMT 1st February, and the highest surge occurs on the Netherlands coast which is leeward of the wind field.

Fig. 4 is a diagram having the same format as Fig. 2, but for the February 1953 surge. The surge-height bar graph, offshore surge diagram, and synoptic weather map are sampled at 06 GMT 1st February. The offshore surge diagram was obtained by a full dynamic computation (Ishiguro, 1961), and not by the method described in this paper.

Fig. 4, particularly the wind speed and direction diagrams at the bottom right, show again that a wind field having a steady direction and high speed generates a high surge.

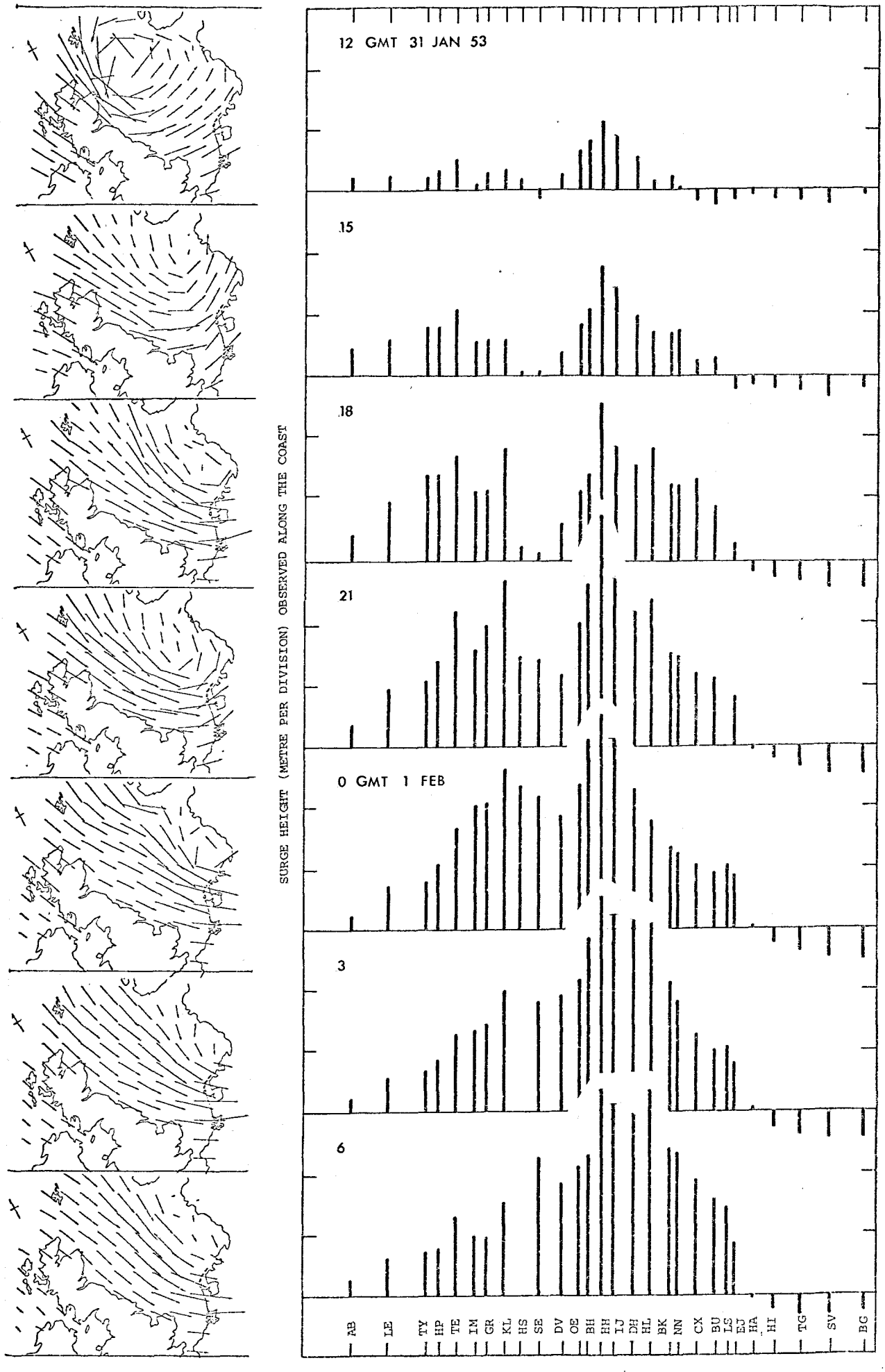

Fig. 3 Wind/pressure field and surge heights observed along the North Sea coast around 1st February 1953.

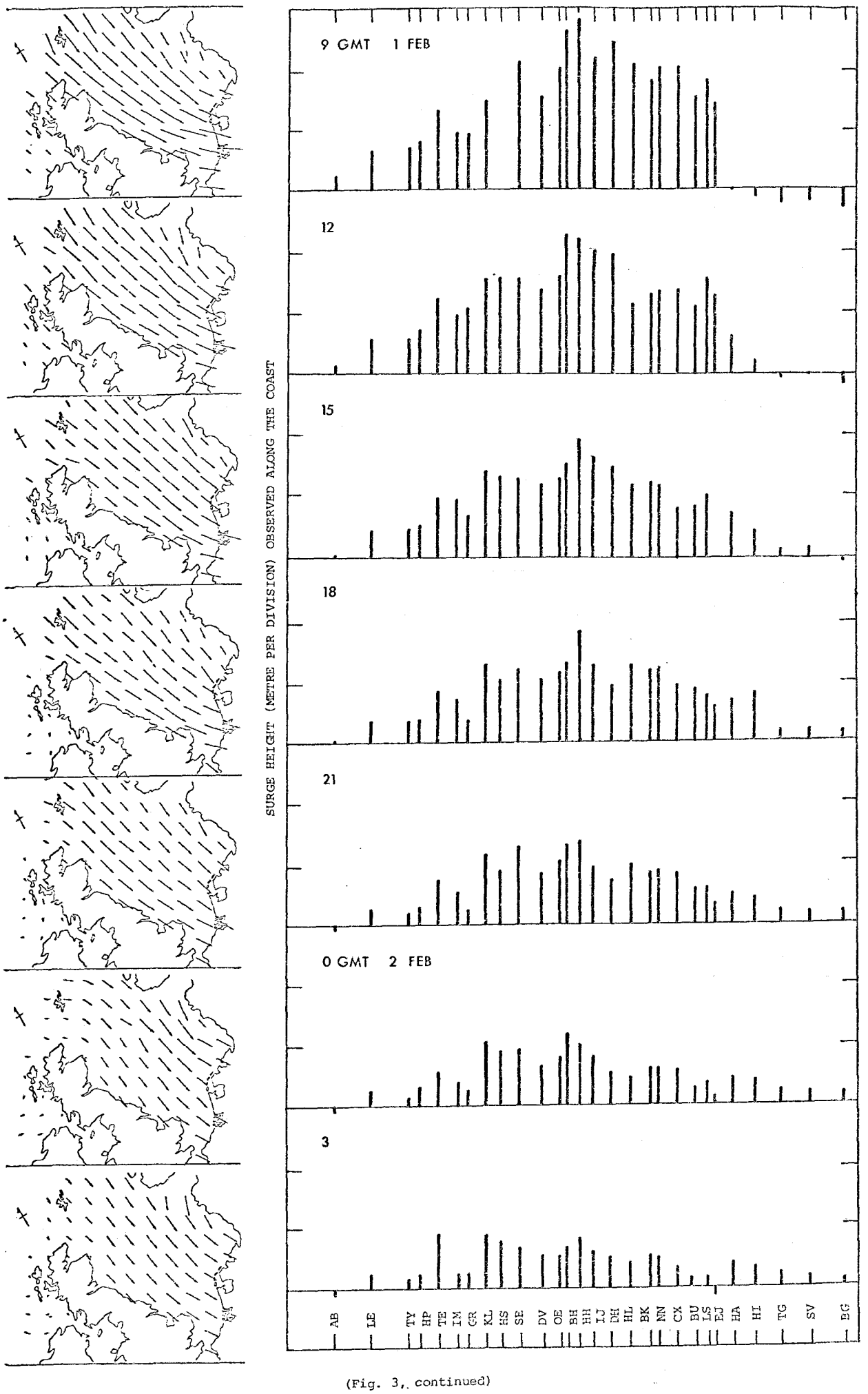

(Fig. 3,. continued)

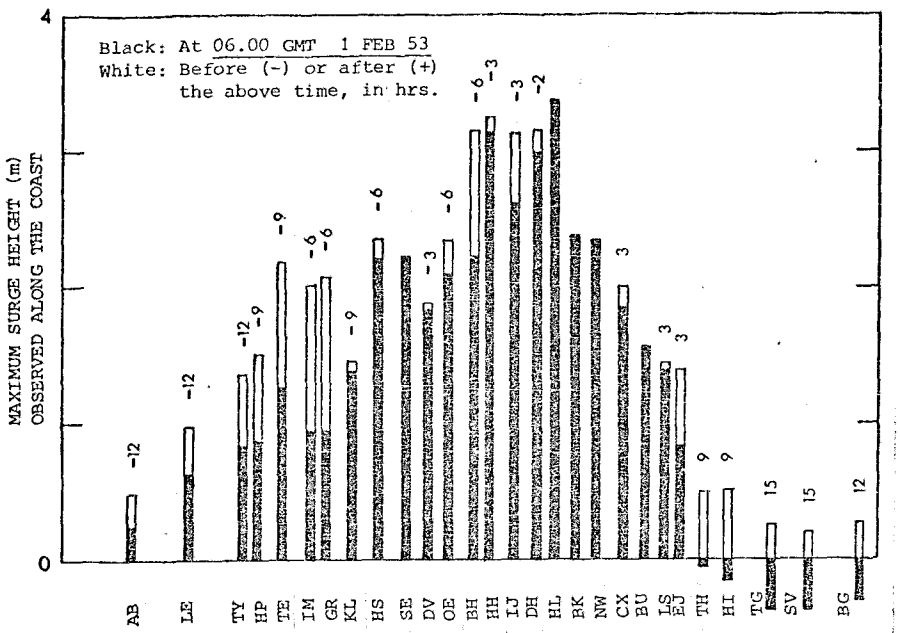

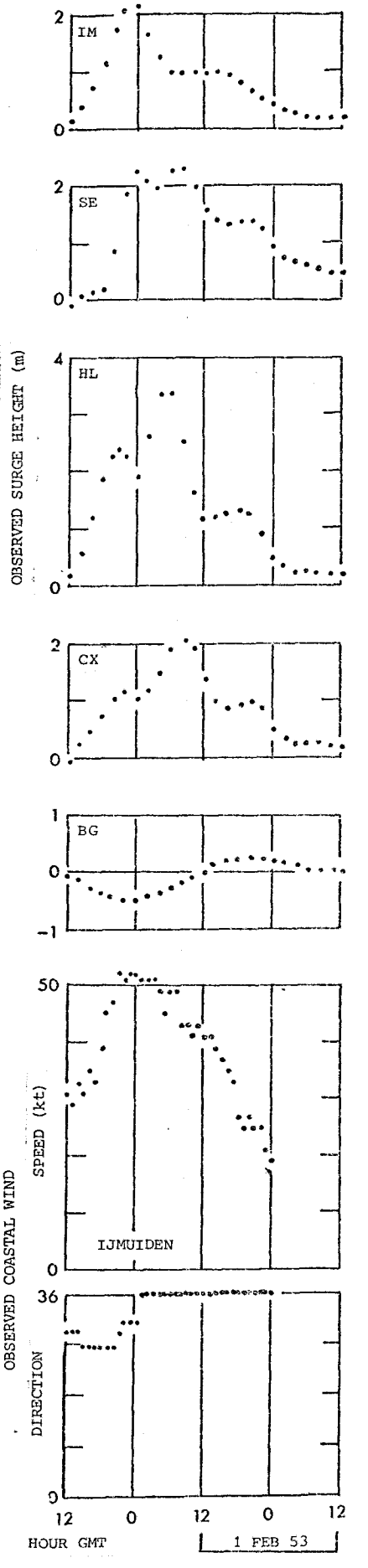

SURGE AT
06.00 GMT 1 FEB 53

COMPUTED BY
Ishiguro (1961)

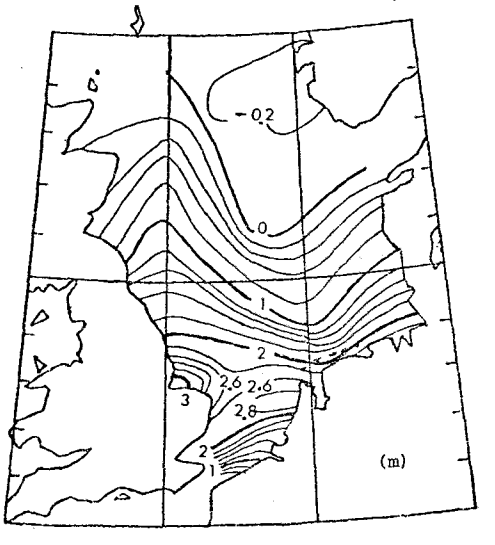

SURFACE PRESSURE AND
WIND OBSERVED AT
06.00 GMT 1 FEB 53

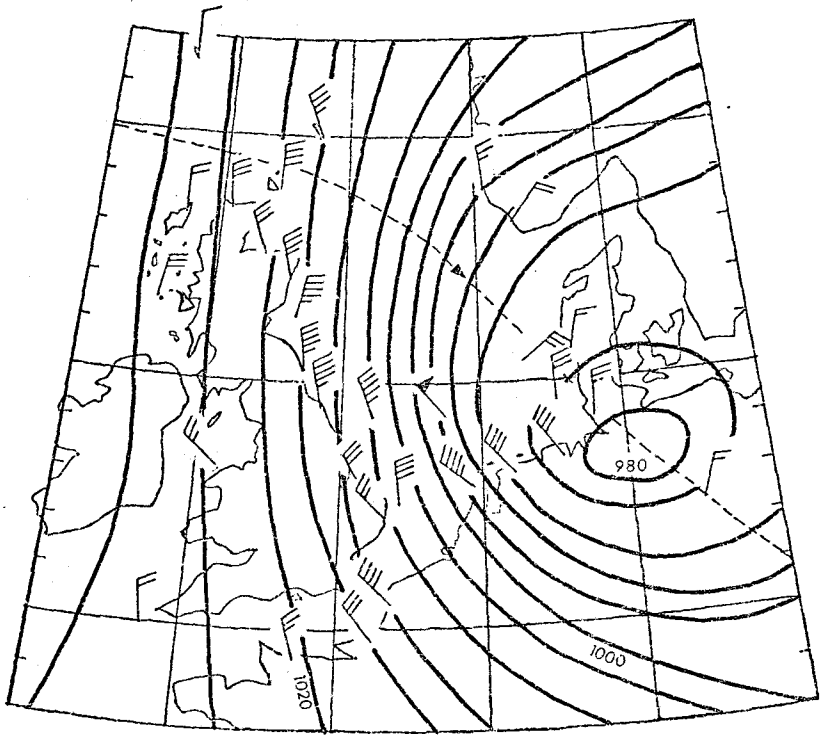

Fig. 4 Summary diagrams of the surge on 1st February 1953.

2.3 44 surge cases in 1898-1956

Fig. 5 illustrates a relationship between a wind/pressure field with a depression centre (shown by a large circle) and a high positive surge (a shaded area) in the North Sea. The North Sea is represented by solid lines, isobars by curved lines, and wind direction by arrows.

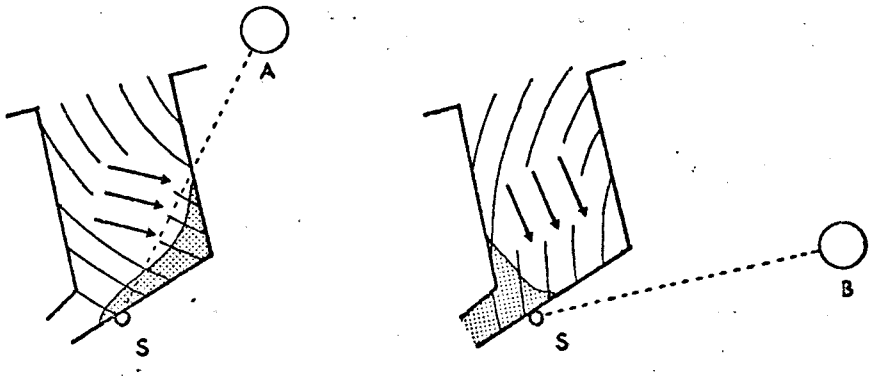

Fig. 5 Schematic representation of two extreme positions (A and B) of the depression centre of a storm which generates a high surge along the coast including station (S).

Assuming that the isobars form concentric circles around the depression centre, the area in which a high surge occurs and the position of the depression centre can be related. If a certain station (S) is in the area, the position of the depression centre for which a wind/pressure field generates a high surge at the station is limited to a certain range of directions seen from the station. As shown in Fig. 5, such a range of directions for station (S) will be angle ASB.

Fig. 6 shows evidence of this theory. Each dot (with case reference number) shows the position of the depression centre of a storm at the time when a surge greater than 160 cm was recorded at Hellevoetsluis. This shows that most of these 44 storms formed quasi uniform steady wind/pressure fields as defined in this paper, and that such fields generate high surges.

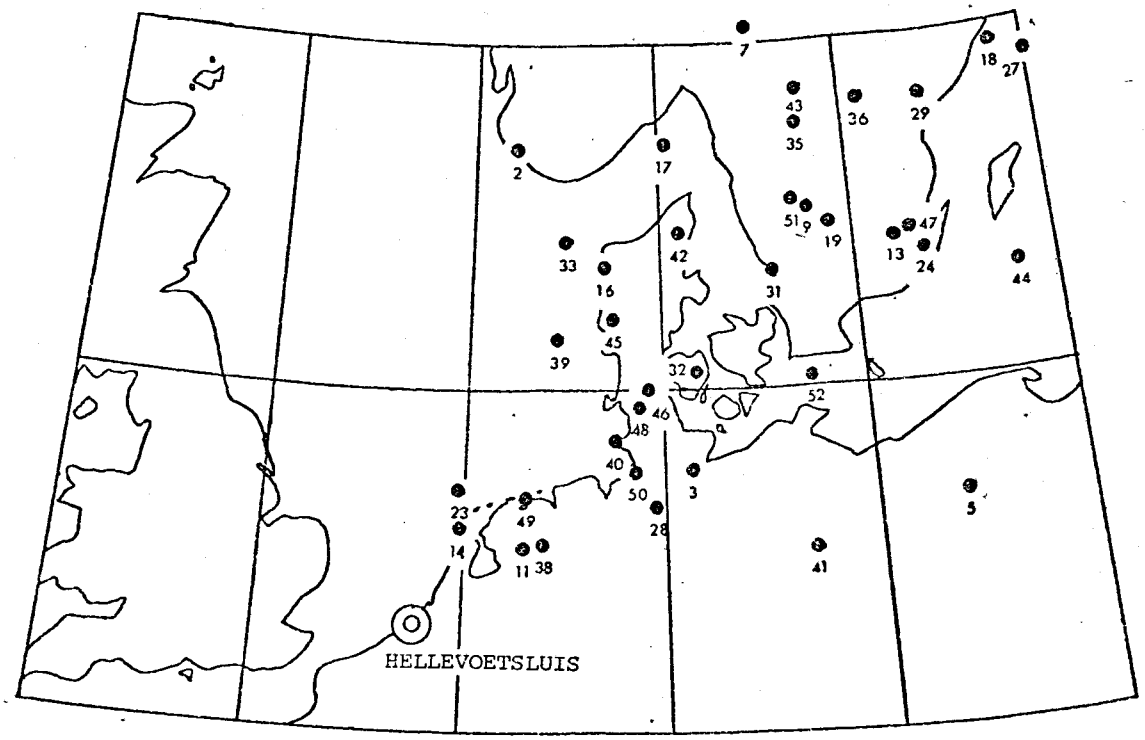

Fig. 6 Positions of depression centres of storms which generated high surges at Hellevoetsluis, 1898-1956.

The record of high surges at Hellevoetsluis (1898-1956), and the record of tracks of depression centres corresponding to the surge cases, have been collected by the Netherlands Delta Committee (1960) for their study subject which is different from the author's. Fig. 6 has been obtained by the author, by combining the data in the above two records, following the idea shown in Fig. 5. A few cases in the original records have been omitted from Fig. 5, since it is difficult to determine the positions of their depression centres.

3. FORMATION OF A QUASI UNIFORM STEADY WIND/PRESSURE FIELD AND SAMPLING

As shown by the examples in the previous chapter, a high surge in a semi-closed sea is generated by a quasi uniform steady wind/pressure field (defined on page 5). Fig. 7 illustrates some possible variations of positions of a storm system relative to the sea. In all the cases, except for e, such a field would be formed, if the size of the storm system is large compared with the sea, and if the system changes slowly, or moves slowly. By interpreting the generation of a high surge in this way, the high surge and storm system can be related more simply and clearly.

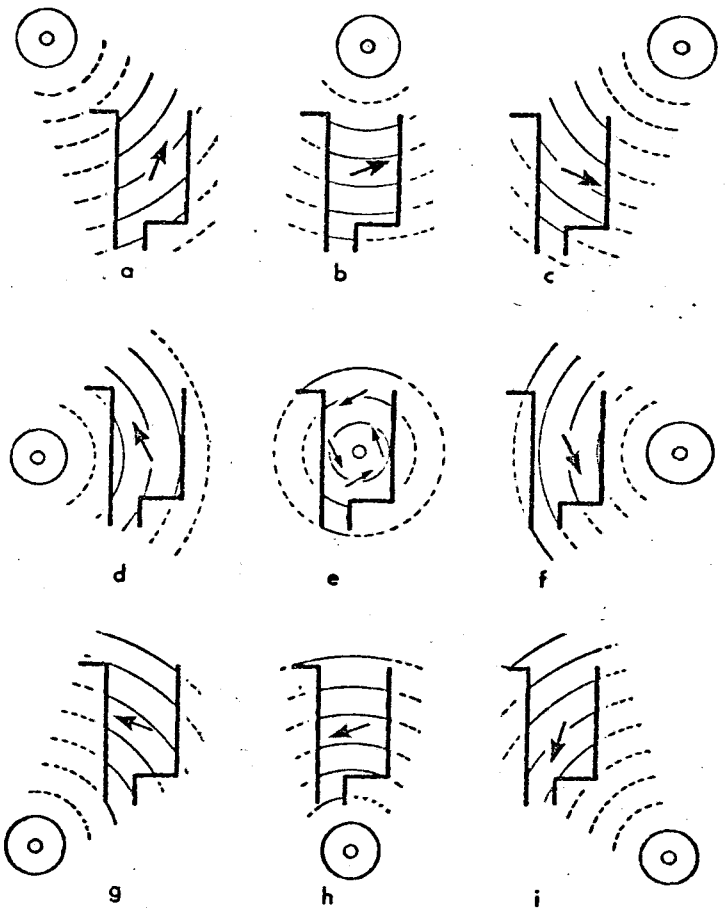

Fig. 7 Variation of positions of a storm system relative to a semi-closed sea (thick lines). A circle shows a depression centre, curved lines show isobars, and an arrow shows a wind direction.

Fig. 8 illustrates the development of a quasi uniform steady wind/pressure field (1st row), and the generation of a high surge (2nd row) both in a 'real' situation. This also illustrates a sampled wind/pressure field for the computation in the method (3rd row), and the computed surge (4th row). In the real wind/pressure field, a duration, in which the wind direction is almost steady, and at the same time, the wind speed is high is sampled as a quasi uniform steady wind/pressure field. This is simulated in the method by a wind/pressure field having a constant wind direction, wind speed, pressure direction and pressure gradient, all of which are averaged over the duration.

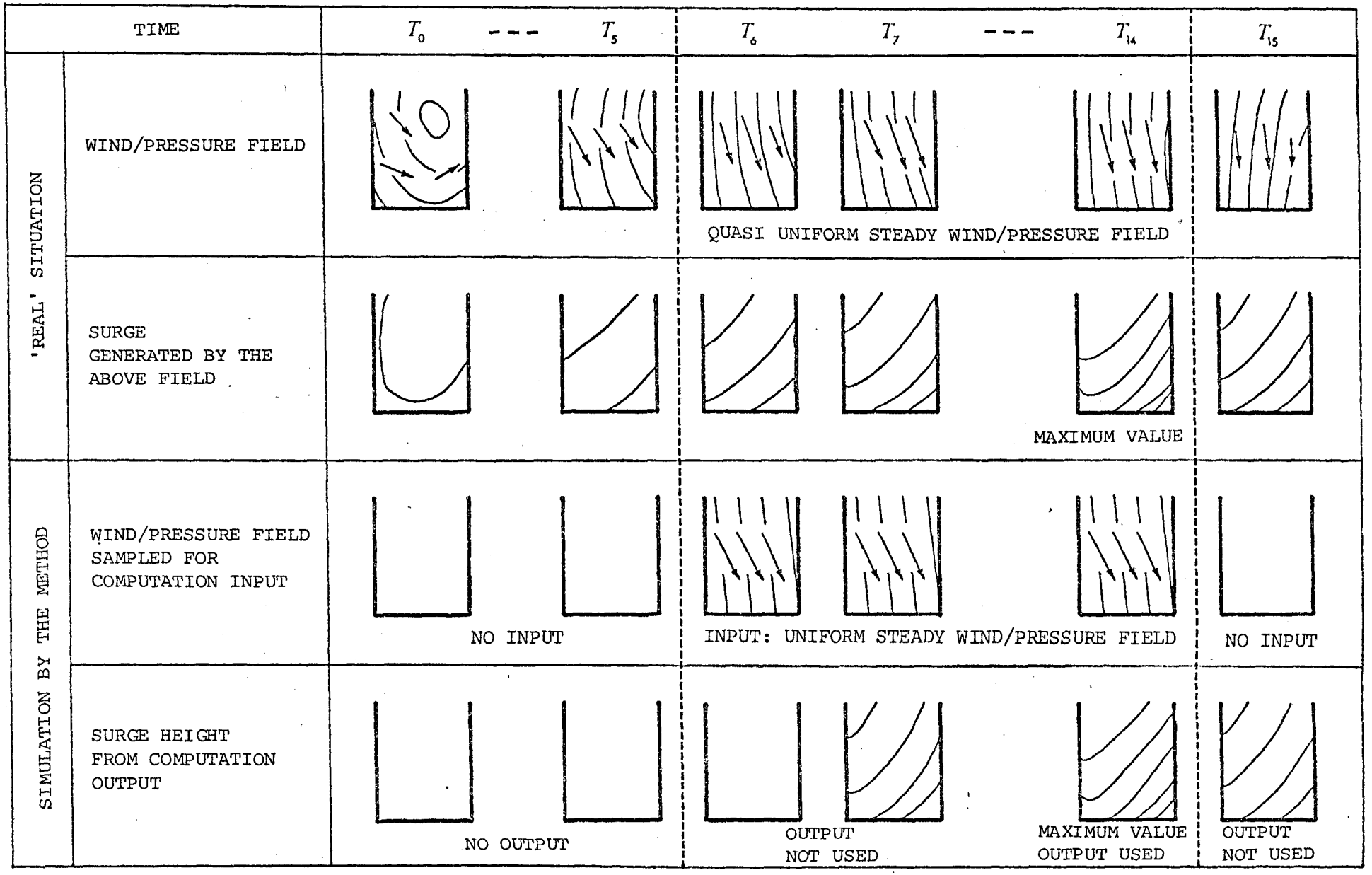

Fig. 8 Surge generated by a 'quasi uniform steady wind/pressure field', and its simulation by the method. Thick lines: sea area (the topography in the model is not simplified). Thin lines in the 1st and 3rd rows: isobars. Thin lines in the 2nd and 4th rows: surge contours. Arrows: wind vectors.

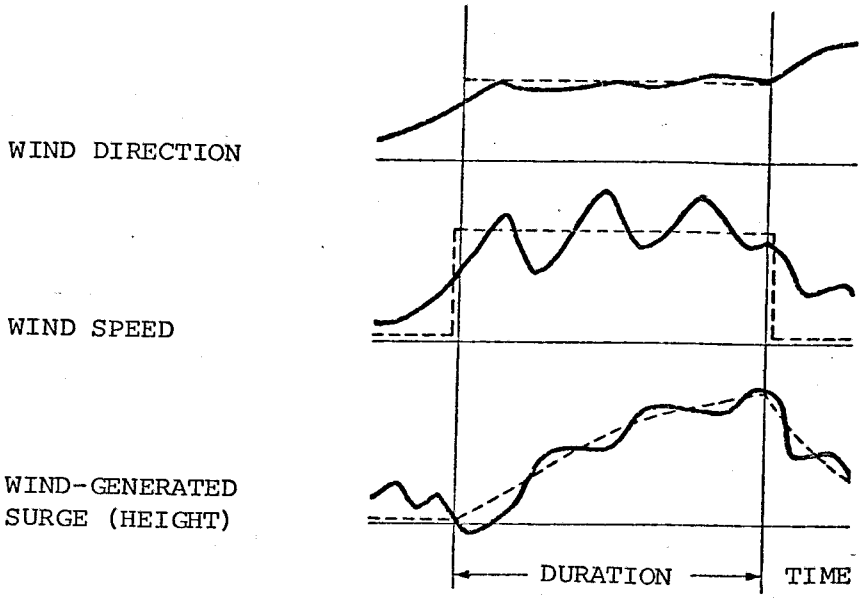

Fig. 9 'Real' wind and wind-generated surge (solid lines); and a simulated wind and wind-generated surge (dotted lines).

A duration in which the wind direction is almost steady, and at the same time, the wind speed is high is selected as a 'quasi uniform steady wind/pressure field'. Wind direction and speed averaged over the duration is used for a simulated wind field in the method. Pressure field and pressure-generated surge are treated in a similar way.

Fig. 9 illustrates the same relationships between the fields and surge as in Fig. 8, but the time variations of the wind direction, wind speed and wind-generated surge at a point in the sea. The pressure direction, pressure gradient and pressure-generated surge have similar relationships.

The representation of a quasi uniform steady wind/pressure field, which in fact varies with time and space to some degree, by a constant field produces an error. However, the error reduces in the maximum value of a high surge, since the dynamic system of the sea generally responds to an average value of the time-and-space varying external forces.

As a wind/pressure field dealt with in the method is constant, this can be represented by only three factors: wind direction, wind speed and duration; or pressure-direction, pressure gradient and duration (the same as the duration of the wind field).

The three factors (either the wind or pressure data) can be sampled from forecast wind/pressure data in the form shown in Fig. 8 or 9 (or equivalent digital data). Practical procedures for sampling depend greatly on the form of available forecast data. Generally, a duration in which the wind direction (or pressure direction) is almost steady, and at the same time, the wind speed (or pressure gradient) is great must be found first, then each value should be averaged over the duration.

4. SURGE PREDICTIONS

The frequency of occurrence of surge heights exceeding a certain level at a point in the sea area generally reduces, if the reference level is increased. If the frequency is fixed, the reference level varies from point to point considerably. Since the author is interested in surges on the scale of the whole North Sea, it is convenient to classify surges into two categories by referring to their frequency of occurrence, rather than surge heights:

Daily surges

Surges occurring quite frequently in a season; and

Long-term extreme surge

Surge occurring only once in many (say 50) years.

Then, two types of surge prediction are considered in the method:

Type-A Daily surge prediction; and

Type-B Long-term extreme surge prediction.

Both the types of prediction are based on the finding that a high surge (positive and negative) in a semi-closed sea (like the North Sea) is generated by a quasi uniform steady wind/pressure field (defined and confirmed in chapter 2). Such a field can be represented by a uniform steady field and indicated by only three factors (chapter 3).

A set of four water-level responses at each point in the North Sea is computed from the surge dynamic equation (or a model). Two of them are responses to two uniform steady wind fields applied in orthogonal directions, and the other two are those for similar pressure fields. Each field is suddenly applied to the sea in a calm state. The responses are expressed in a generalized form for an arbitrary intensity of the fields.

Combining the above three factors and four responses, the maximum surge height at each point can be obtained for each specific surge case. Since the values of the responses are independent from each surge case, the set of responses can be used repeatedly.

For Type-A prediction, the three factors are obtained from forecast wind/pressure data. For Type-B prediction, only an extreme wind speed is available. Therefore, a technique to determine the maximum surge height, only from the extreme wind speed, has been developed.

The method (both Type-A and Type-B) offers the prediction of the maximum surge height at each point in each surge case, and not the time-varying height.

Details of Type-A and Type-B prediction procedures are explained in the following sections separately.

4.1 Type-A prediction

Fig. 10 shows an outline of Type-A prediction procedure.

Before the operation, sets of water-level responses, X, Y, J, K, have to be computed from the surge dynamic equations (or model). X and Y are responses to two uniform wind fields in the x and y directions respectively. J and K are responses to two uniform pressure fields in the x and y directions respectively. Each field is suddenly applied to the sea in a calm state, and the value of response at the end of duration of d is obtained. Each value is given in a generalized form so that this can be used with an arbitrary wind speed or pressure gradient. Since the values depend on duration d, different sets of X, Y, J, K are required for different d's in principle. In practice, about 10 sets with logarithmic intervals of d have been found to be sufficient. Examples of X, Y, J, K indicated by diagrams are shown in Figs. 11 and 12, although their numerical sets are also available.

A surge prediction starts with finding a quasi uniform steady wind/pressure field from a forecast wind/pressure data, and indicating it by the three factors: d, θ_d and U_d. From U_d and θ_d, the pressure gradient, $\partial p/\partial x$ or $\partial p/\partial y$, and its direction (relative to the wind direction) β, can be determined, by assuming a certain relationship between a wind field and a pressure field (see Appendix 2).

Next, an appropriate set of X, Y, J, K is selected by d. Then ζ_{wx} and ζ_{wy} (in Fig. 10) are determined by applying U_d to the selected X and Y; and ζ_{px} and ζ_{py} are determined by applying $\partial p/\partial x$ or $\partial p/\partial y$ to the selected J and K. Finally the resultant surge height ζ is determined by the last equation in Fig. 10.

Table 1 (pages 24 and 25) shows an example of a programme for the operation shown in Fig. 10. The programme has been written in a basic language so that this can be applied to a small table-top computer. This example contains the values of X, Y, J, K for 30 coastal stations along the North Sea coast. The same programme, but containing 60 offshore stations in the North Sea, is also readily available.

Figs. 13 and 14 show examples of computed and observed surge heights along the North Sea coast (see the footnote on page 5, for the format). Although computed data are available for both coastal and offshore stations, coastal data only are compared, because observational data offshore are not available. In each figure, the envelopes of the computed and observed bar graphs should be compared. Note, stations in the two types of graph are not exactly the same.

Fig. 13 shows the 1st February 1953 surge. This is simulated by a single constant field, for which values are shown in the top-left of the upper diagram. X+C indicates that the values in the X diagram have been corrected by a method described in Appendix 3.

Fig. 14 shows the 3rd January 1976 surge. The wind/pressure field for this surge case was simulated by two constant fields, since the wind direction was changed considerably without decaying the wind speed. The values of the two fields are shown in the top-left of the upper diagram. The computed surge heights derived from the first and second fields are shown by black bars and white bars respectively. In the lower diagram, a surge height observed at the sampled time is shown by a black bar. The maximum surge height occurring at each station during this surge case is shown by a white bar.

As the stations for the computed and observational data are not all common, only those which are common can be compared directly. When the above two examples are compared in this way, the RMS error is 52 cm. If the data for Cuxhaven and Büsum, which have a strong local effect, are excluded, the RMS error is 46 cm. For both the cases, the RMS errors correspond to about 10% of the maximum value involved. Therefore, the prediction method is reasonably accurate, though not perfect.

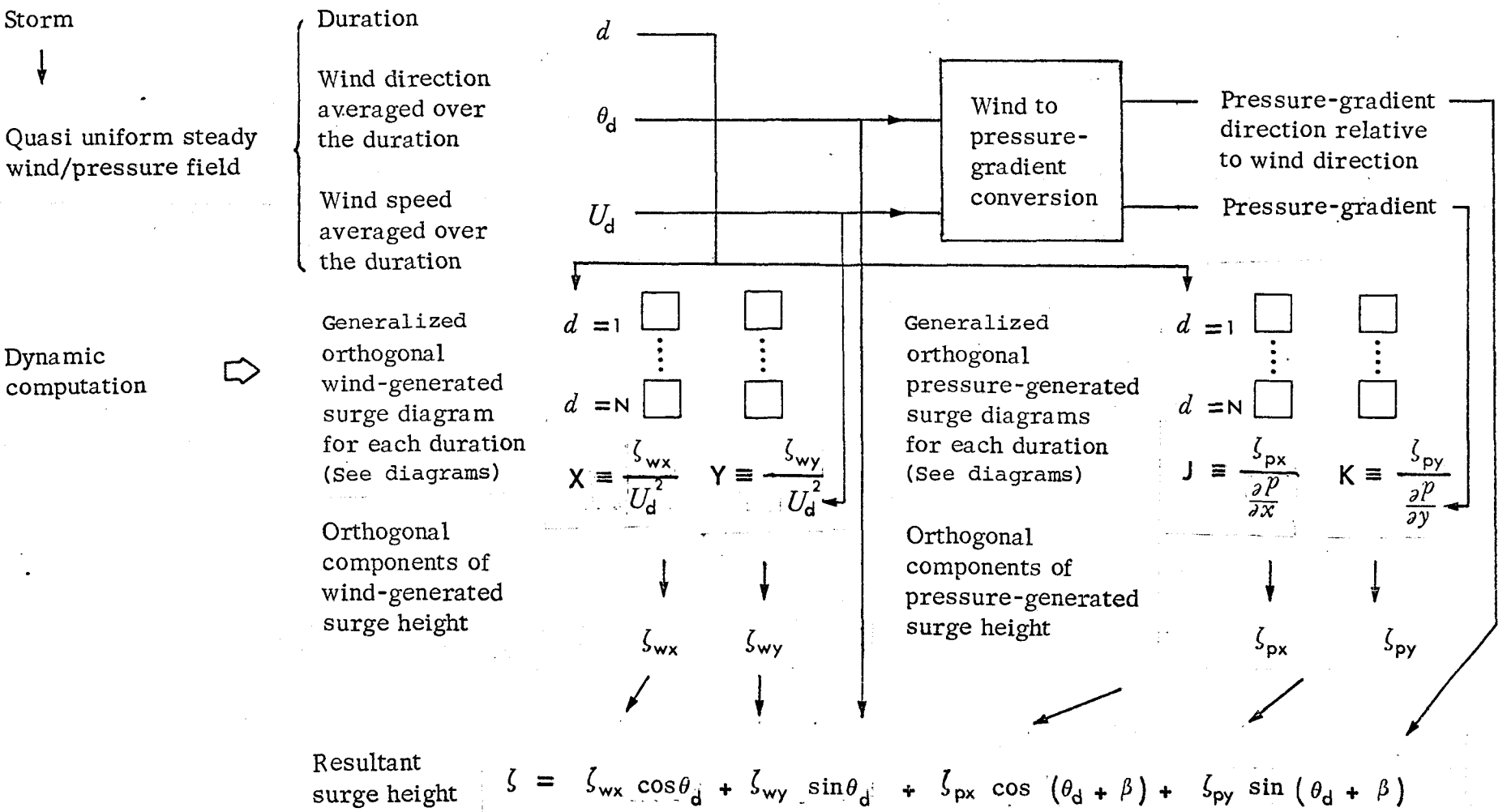

Fig. 10 Outline of daily-surge prediction procedure, Type-A.

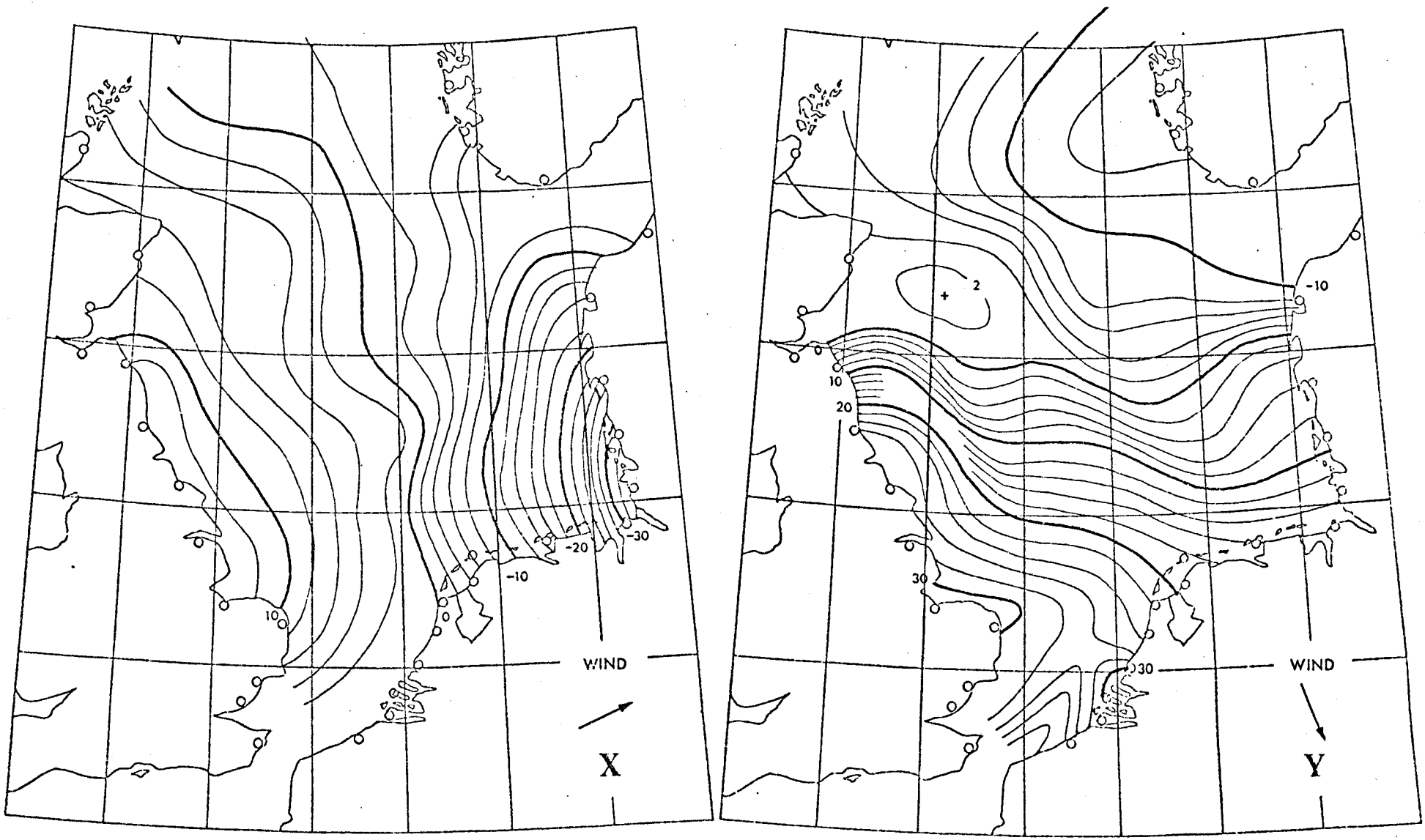

Fig. 11 Example of the generalized water-level responses, X and Y, to the orthogonal uniform wind fields which is suddenly applied to the North Sea in a calm state. Line value: × 0.01 cm/(m/s)². Diagrams for the duration of 20 hours only are shown.

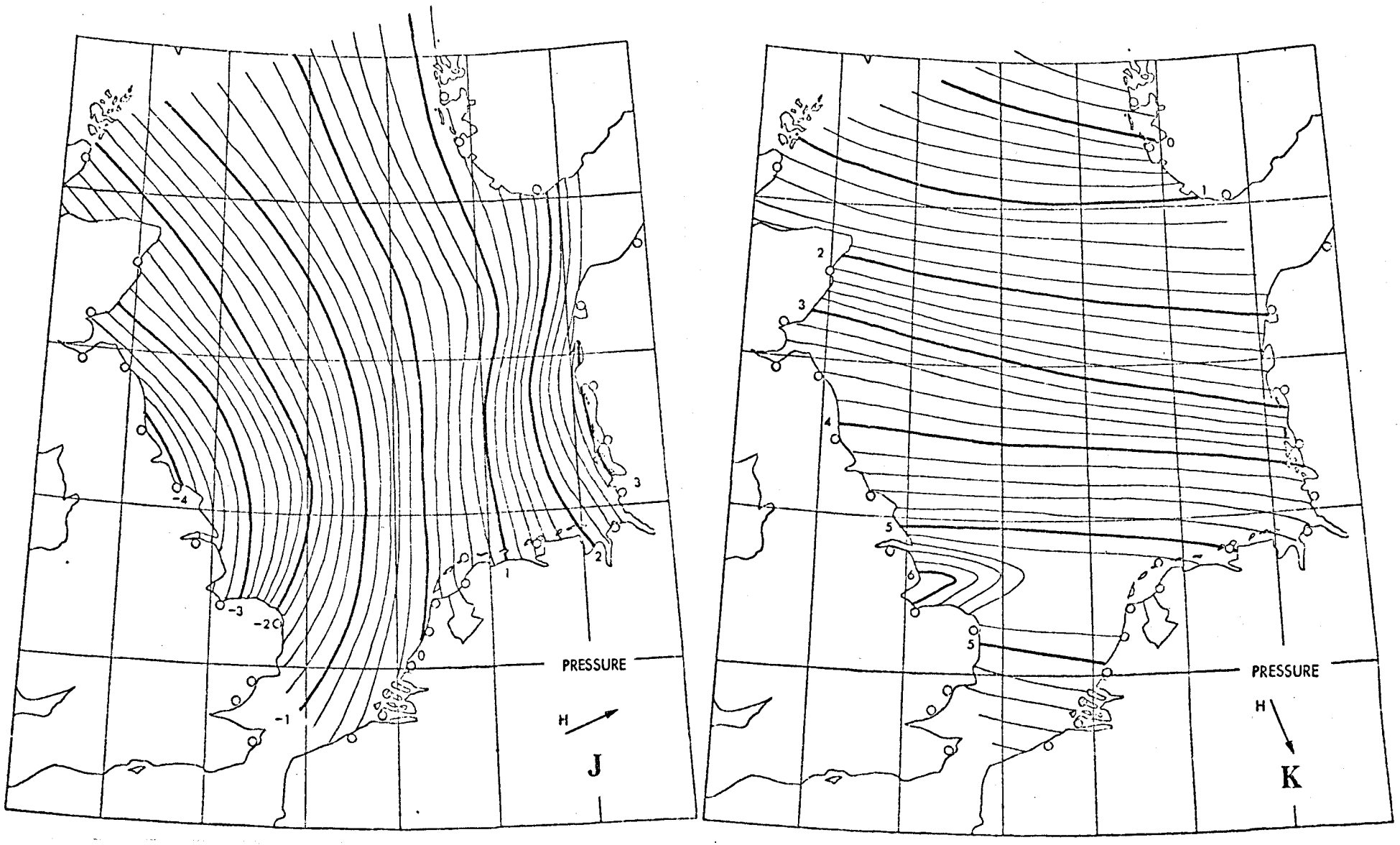

Fig. 12 Example of the generalized water-level responses, J and K, to the orthogonal uniform pressure field which is suddenly applied to the North Sea in a calm state. Line value: cm/(mb/100 km). Diagrams for the duration of 20 hours only are shown.

Table 1 Programme for Type-A prediction.

In Fig. 10			
d	T	Duration	hours
θ_d	D	Wind direction averaged over the duration	degrees
U_d	U	Wind speed averaged over the duration	m/s
ζ_{wx}/U_d^2	X	Generalized water-level response to a uniform wind field in x direction	cm/(m/s)^2
ζ_{wy}/U_d^2	Y	y direction	cm/(m/s)^2
$\zeta_{px}/\frac{\partial p}{\partial x}$	J	Generalized water-level response to a uniform pressure field in x direction	cm/(mb/100 km)
$\zeta_{py}/\frac{\partial p}{\partial y}$	K	y direction	cm/(mb/100 km)
α	A	Angle between wind direction and isobar	degrees
β	B	Angle between wind direction & pressure-gradient direction	degrees
ζ_w	W	Wind-generated surge height	cm
ζ_p	P	Pressure-generated surge height	cm
ζ	R	Resultant surge height	cm
-	I	Station number	-

α is not shown in Fig. 10.

Programmes for coastal and offshore stations are the same, but they are recorded on separate parts of a cassette tape for convenience.

As data (X, Y, J, K) in the programme have specific values for each station and for each duration, they are also recorded on a separate section of the tape.

The programme shown on the next page is an example of a particular section of the tape containing the specific values for 30 coastal stations for a duration.

To use,

(1) Select the part required 'coastal' or 'offshore';

(2) Select the section for the required duration T; and

(3) Specify wind speed U and wind direction D by using the computer keyboard.

The output will print out the value of W, P and R for each station with its reference number I.

Programme for Type-A prediction (Table 1, continued)

```
10 LET T=20
12 LET U=
14 LET D=
30 OPEN 2,4
35 CMD 2
38 PRINT#2,"AAP COASTAL SURGE"
39 PRINT#2,"T=";T;"(HR)";"   U=";U;"(M/S)";"   D=";D;"(DEG)"
40 PRINT#2,
42 PRINT#2,"ST","W(CM)","P(CM)","R(CM)"
45 CLOSE 2
50 FOR I=1 TO 30
51 DATA -5,-3.7,-2.2,1.3,   -7.4,-1.8,-2.6,2.3,   -9.2,-1.6,-3.4,3.2
52 DATA -10,0.0,-4.0,3.6,   -11.8,7,-3.6,3.6,   -14.5,26,-4.5,4.1
53 DATA -14,28.3,-4.5,4.7,   -14.3,28.3,-3.8,5.6,   -14.2,31,-3.3,6
54 DATA -9,30.5,-1.8,5.1,   -5.5,28,-1.5,4.6,   -4.2,28,-1.5,4.2
55 DATA 0.0,25,-.4,4.3,   0.0,30,-.2,4.5,   0.0,30,-.3,4.7
56 DATA 0.0,30,-.1,5,   0.0,23.5,-.1,5.2,   -.3,21.8,.1,5.2
57 DATA 4,19.3,.5,5.2,   6.3,18.3,.5,5.2,   14.5,16,1.5,5
58 DATA 30.5,15.8,2.5,4.8,   35,13.3,2.9,4.3,   31.2,9.3,3.2,3.7
59 DATA 25,6.3,3.2,2.8,   16,-7.8,2.7,2,   7.5,-11.5,3.4,1.4
60 DATA 7.2,-11.5,1.9,1,   4.8,-12.5,1.2,.2,   3.2,-10.5,1.4,-1.5
200 READ X,Y,J,K
210 LET X=X*(U/10)↑2
212 LET Y=Y*(U/10)↑2
214 LET J=J*(.653*U↑2+14.37*U+12.2)*.008192
216 LET K=K*(.653*U↑2+14.37*U+12.2)*.008192
220 LET A=22
222 LET B=90-A
224 LET C=D+112
230 LET W=X*COS(C*π/180)+Y*SIN(C*π/180)
232 LET P=J*COS((C-B)*π/180)+K*SIN((C-B)*π/180)
234 LET R=W+P
240 W=INT(W+.5)
242 LET P=INT(P+.5)
244 LET R=INT(R+.5)
300 OPEN 3,4
302 CMD 3
304 PRINT#3,I,W,P,R
306 CLOSE 3
318 NEXT I
```

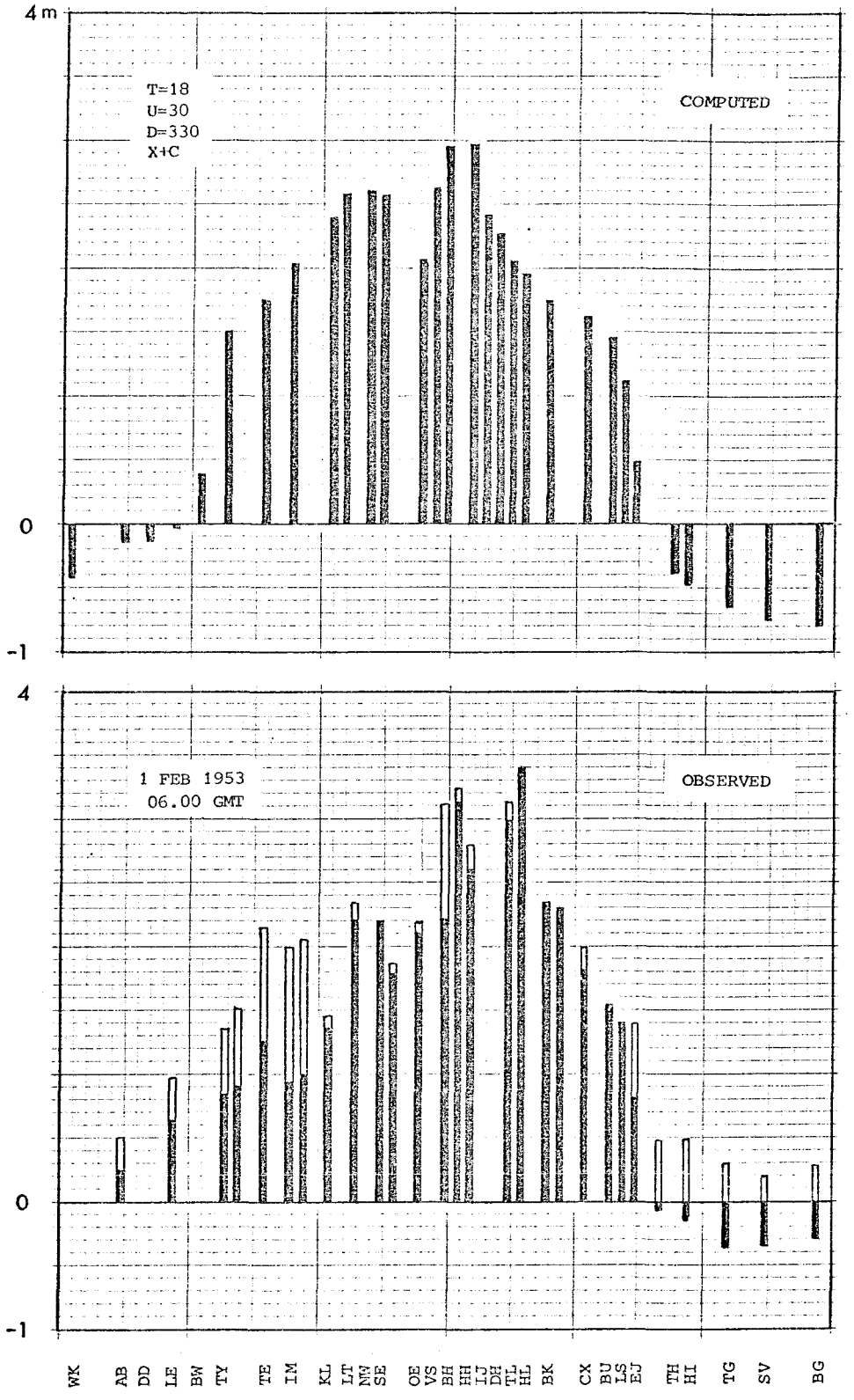

Fig. 13 Comparison of surge height computed by Type-A prediction procedure, with surge height observed along the North Sea coast, at 06.00 GMT, 1st February 1953. The envelopes of the two graphs should be compared. See the text (page 19) for explanations.

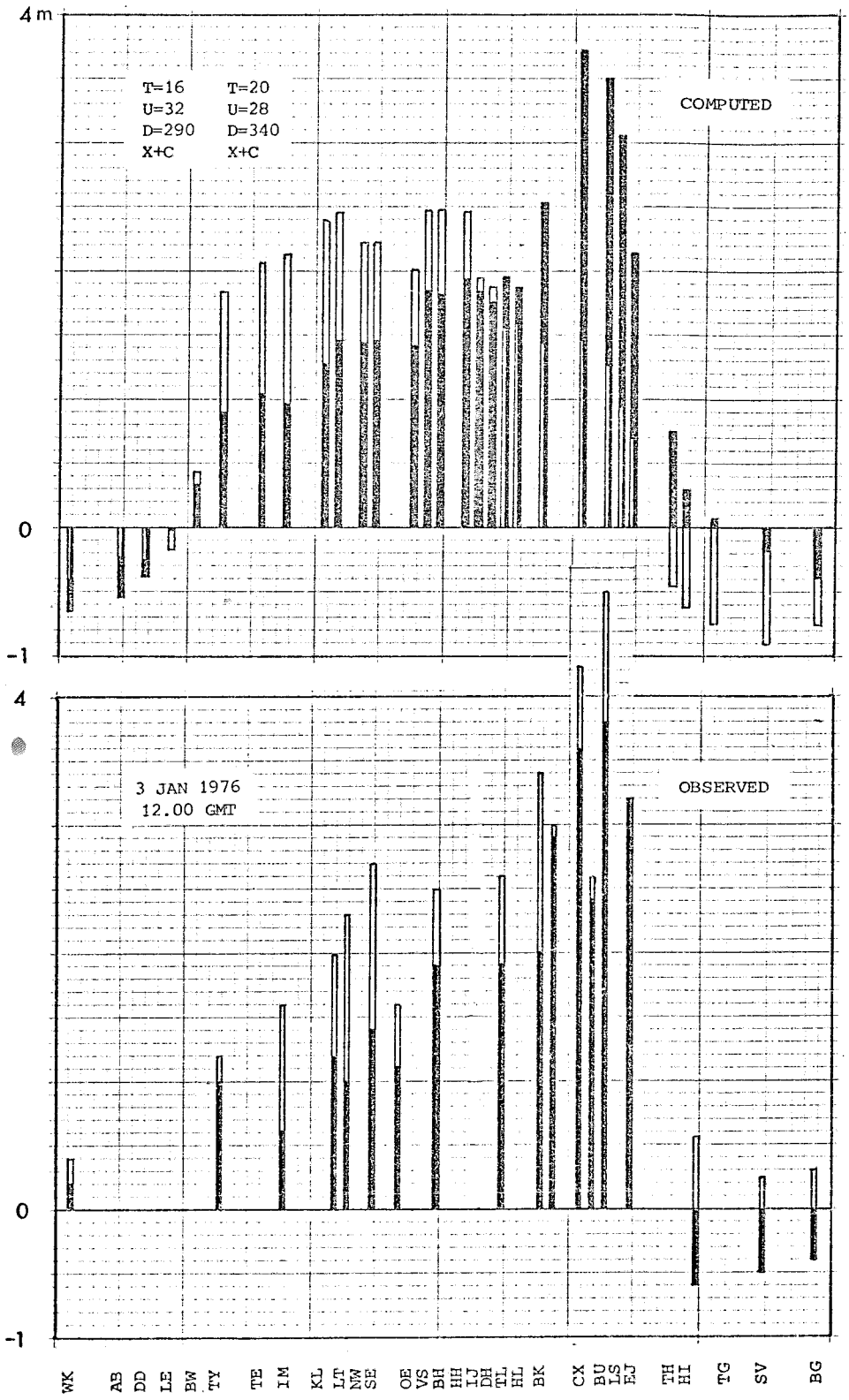

Fig. 14 Comparison of surge height computed by Type-A prediction procedure, with surge height observed along the North Sea coast, at 12.00 GMT, 3rd January 1976. The envelopes of the two graphs should be compared. See the text (page 19) for explanations.

4.2 Type-B prediction

A long-term extreme surge can be predicted in the same way as Type-A prediction procedure, if the predicted long-term extreme values of a wind direction, wind speed and duration are available. In practice, however, only a once-in-50 year extreme wind speed is available for the North Sea area, without other information. Type-B prediction procedure has been developed for this situation.

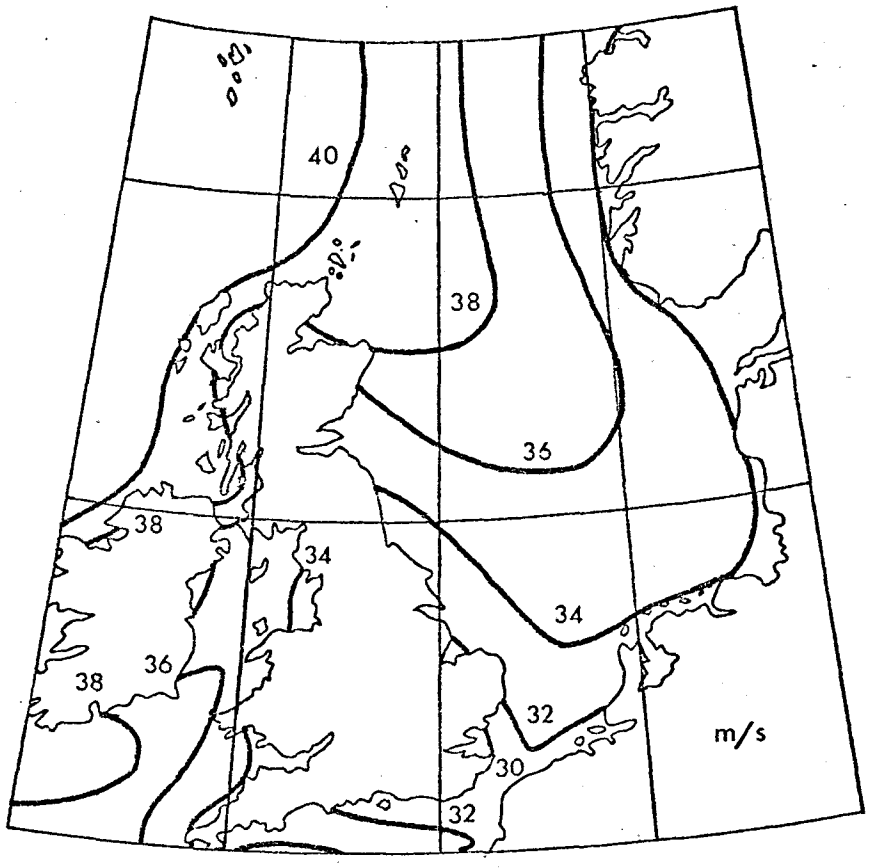

Fig. 15 Once-in-50 year extreme wind speed over the North Sea area (Shellard, 1974).

Fig. 15 shows the once-in-50 year extreme wind speed for the North Sea area, produced by Shellard (1974, published in 1977), and the only one of this kind at the moment. The extreme wind speed (10 m above the sea surface, hourly-mean value) ranges from 30 to 40 m/s in the sea area. Shellard recommends the hourly-mean value be reduced, if this is applied for a longer duration than one hour. He found (1975) the reduction factors for several durations, as shown by circles in Fig. 16, from independent observational data with a statistical treatment.

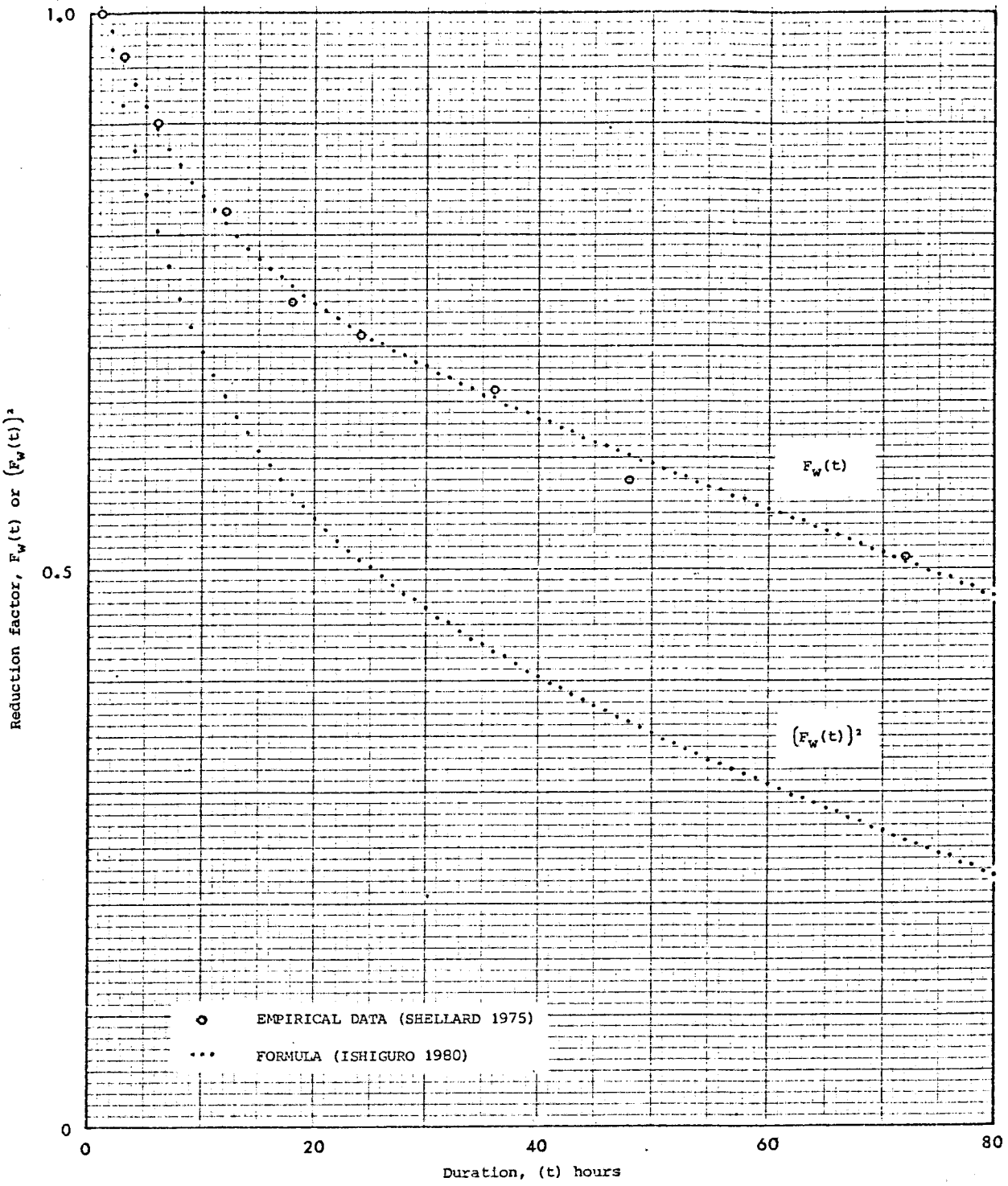

Fig. 16 Reduction factors for the once-in-50 year extreme wind (hourly-mean speed), when it is used for a duration longer than one hour.

The author has found a single formula:

$$F_w(t) = 0.79 - 0.00394t + 0.25e^{-0.11t} \qquad (t \text{ in hours})$$

which covers all Shellard's reduction factors. The upper dotted line in Fig. 16 shows the values of the reduction factor with hourly intervals, derived from the formula. The lower line shows the square of the reduction factor, and is useful for cases involving the square of the wind speed. The numerical table of these values are given in a separate paper (Ishiguro, 1980).

According to the above information, the predicted once-in-50 year extreme wind speed reduces following the reduction factor of $F_w(t)$ which is a function of time (duration). On the other hand, a surge generated by a suddenly applied uniform wind field increases (positively or negatively) with time. Therefore, a surge, generated by a suddenly applied uniform wind field having a predicted wind speed with a certain duration, depends on the duration. Generally, the surge height becomes maximum (positive or negative) at a certain duration. Fig. 17a illustrates these relationships.

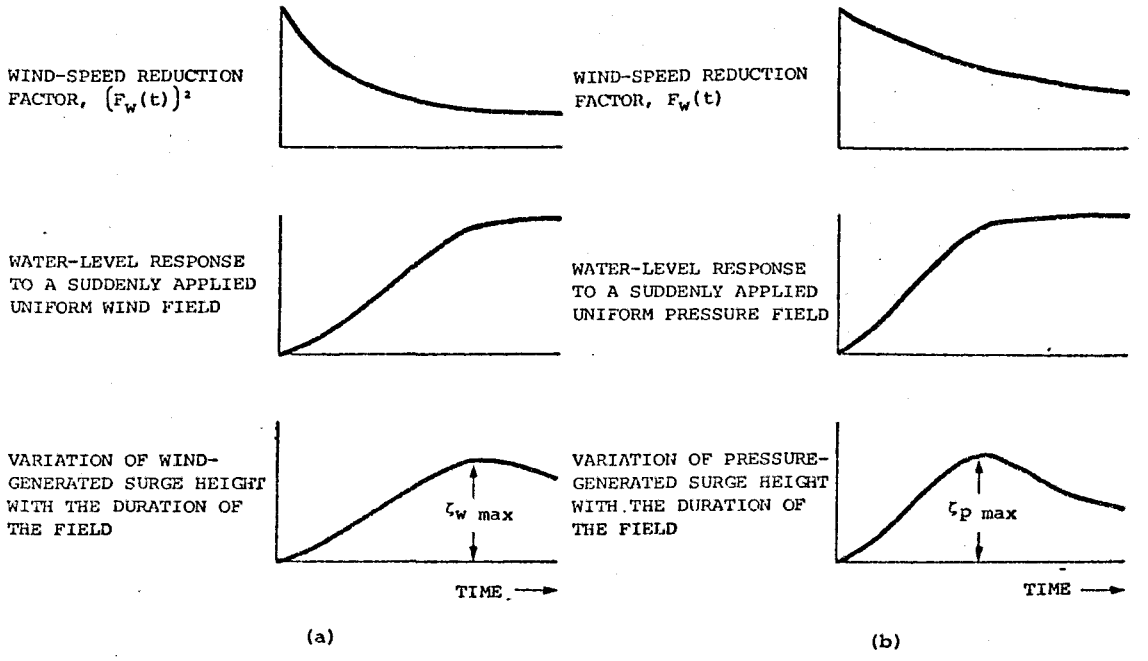

Fig. 17 Relationships between the wind-speed reduction factor, water-level response to a suddenly applied uniform field, and a surge height variation with the duration of the field. (a) Wind-generated surge. (b) Pressure-generated surge.

Since the information of a once-in-50 year pressure field is not available, this has to be estimated from the predicted once-in-50 year extreme wind field, assuming a certain relationship between the two fields. For example, the pressure gradient and its direction can be estimated from the wind speed and direction, although the absolute values of pressure field cannot be estimated from the wind field data. A pressure gradient determined in this way reduces following the reduction factor of $F_w(t)$ which is again a function of time. A surge generated by a suddenly applied uniform pressure field increases (positively or negatively) with time, but with a different characteristic from the wind-generated surge. A surge generated by a suddenly applied uniform pressure field having an estimated pressure gradient becomes maximum (positive or negative) at a certain duration. Fig. 17b illustrates these relationships.

The maximum surge height finally required is determined by the combination of two types of surge shown in Fig. 17. The maximum surge height, and the conditions which produce this height, greatly vary from point to point in the sea area.

Fig. 18 shows an outline of Type-B prediction procedure, which determines the maximum value of the resultant surge practically. This starts with three types of factors:

(1) Predicted once-in-50 year extreme wind speed;

(2) Water-level responses; and

(3) Wind-speed reduction formula.

(2) has been obtained from the surge dynamic equations (or model), with the conditions that uniform wind fields in orthogonal directions are suddenly applied to the sea in a calm state. (2) is combined with (3). Then the maximum value of the combined factor for each point is determined numerically by varying the duration (t). X and Y in Fig. 18 indicates the maximum values of wind-generated surges in the x and y directions respectively obtained in this way. Fig. 19 is an example of a set of diagrams showing the values of X and Y for the North Sea. J and K in Fig. 18 indicate the maximum values of pressure-generated surges in the x and y directions respectively, obtained in the same way. Fig. 20 is an example of these values.

By applying a predicted once-in-50 year extreme wind speed (hourly-mean value) U_1 to factors X and Y, the maximum surge heights at each point generated by the wind fields in the x and y direction, $\hat{\zeta}_{wx}$ and $\hat{\zeta}_{wy}$, are obtained. Similarly, by applying a once-in-50 year extreme pressure gradient, $\partial p/\partial x$ or $\partial p/\partial y$, which is estimated from U_1, to factors J and K, the maximum surges at each point generated by pressure field in the x and y directions respectively, $\hat{\zeta}_{px}$ and $\hat{\zeta}_{py}$, are determined.

The resultant surge ζ is given by the penultimate formula in Fig. 18, which is a function of ζ_{wx}, ζ_{wy}, ζ_{px}, ζ_{py}, β and θ_w. By specifying the values of the first four parameters from the above information, and by specifying the value of β which is the direction of the pressure field relative to the wind direction, the formula becomes the function of wind direction θ_w only. Therefore, by choosing the value of θ_w so that ζ becomes maximum, the maximum surge height ζ_{max} and the wind direction $\theta_{w\ max}$ which generates such a surge can be determined. The pressure-field data can be derived from the wind-field data, by using a certain relationship (see Appendix 2).

The determination of ζ_{max} and $\theta_{w\ max}$ in the last equation in Fig. 18 can be carried out either by (a) a totally numerical computation (varying the value of θ_w), or (b) by using an analytical formula which determines the maximum value directly. The author uses (b) with a minor simplification. The formula has been described in a separate paper (Ishiguro, 1976).

Table 2 is an example of the programme for the operation shown in Fig. 18, which includes the analytical formula in (b), but excludes the surge-dynamic equations from which the values of X, Y, J, K have been derived. The programme in Table 2 has been written again in a basic language so that this can be processed by a small table-top computer. The same programme can be used for both coastal and offshore stations, although the example shown in Table 2 contains the values of X, Y, J, K and E (see page 35) for each of 30 coastal stations along the North Sea coast. Another set of programmes containing 60 offshore stations is also available.

Fig. 21 shows an example of a once-in-50 year extreme surge predicted by Type-B procedure.

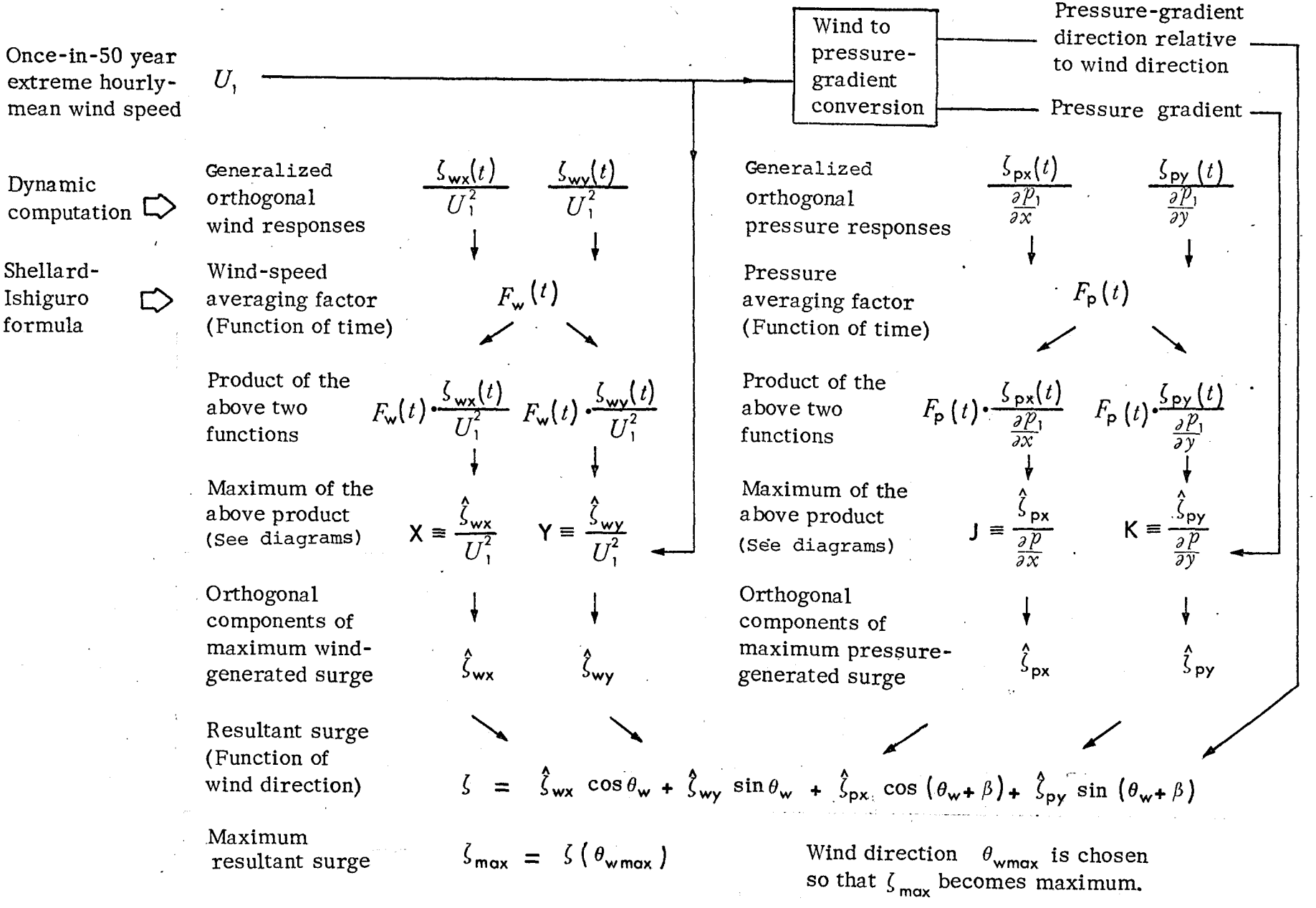

Fig. 18 Outline of extreme-surge prediction procedure, Type-B.

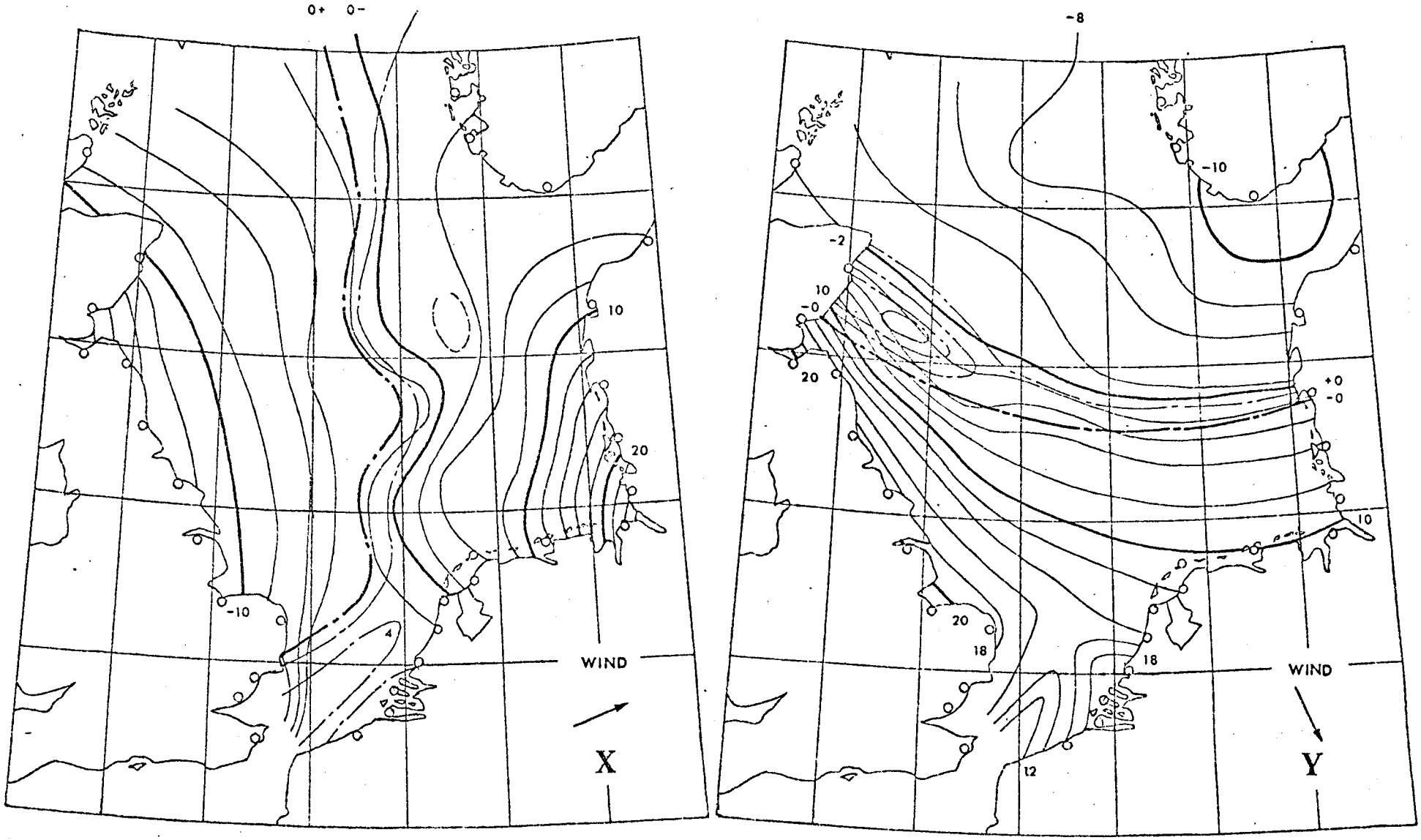

Fig. 19 Example of the generalized water-level responses, X and Y, to the orthogonal uniform wind field which is suddenly applied to the North Sea in a calm state. Line value: × 0.01 cm/(m/s)².

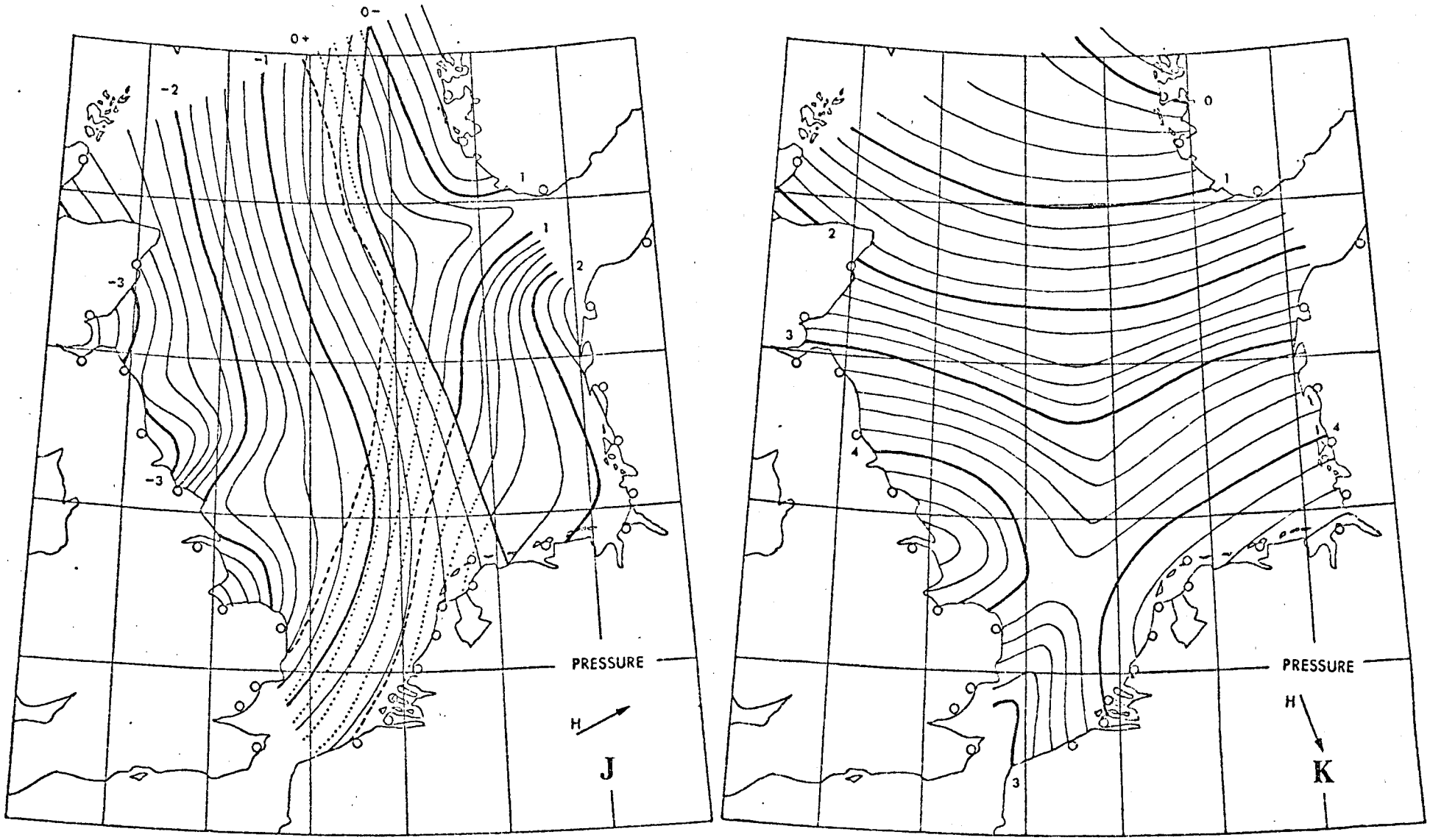

Fig. 20 Example of the generalized water-level responses, J and K, to the orthogonal uniform pressure field which is suddenly applied to the North Sea in a calm state. Line value: cm/(mb/100 km).

Table 2 Programme for Type-B prediction.

In Fig. 18			
U_1	U	Hourly-mean extreme wind speed	m/s
ζ_{wx}/U_1^2	X	Generalized water-level response to a uniform pressure field in x direction	cm/(m/s)²
ζ_{wy}/U_1^2	Y	y direction	cm/(m/s)²
$\zeta_{px}/\frac{\partial p}{\partial x}$	J	Generalized water-level response to a uniform wind field in x direction	cm/(mb/100 km)
$\zeta_{py}/\frac{\partial p}{\partial y}$	K	y direction	cm/(mb/100 km)
α	A	Angle between wind direction and isobar	degrees
β	B	Angle between wind direction and pressure-gradient direction	degrees
θ_{wn}	P	Angle between wind direction and model grid axis	degrees
θ_w	D	Wind direction	degrees
ϵ	E	Direction of model grid	degrees
λ	L	Angle introduced for quadratic selection	degrees
ζ_{max}	R	Maximum resultant surge height	cm
-	I	Station number	-

α, θ_{wn}, ϵ and λ are not shown in Fig. 18

Programme for coastal and offshore stations are the same, but they are recorded on separate parts of a cassette tape for convenience.

An example of the programme for 30 coastal stations is shown on the next page. Equations in Lines 123 to 428 have been derived from the theory described in a separate paper (Ishiguro, 1976).

To use, select an appropriate part first, then specify an extreme hourly-mean wind speed by using the computer keyboard.

If the output of the programme indicates 'CHECK DATA', the values of a set of data (X, Y, J, K) in the line at which the computation stopped might have an illogical combination, and this should be cleared.

The normal output will print out the values of R and D for each station with its reference number I.

```
0 REM "SPECIFY HOURLY-MEAN EXTREME WIND SPEED IN (M/S)"
2 LET U=
4 OPEN 2,4
6 CMD 2
8 PRINT#2,"BBP COASTAL SURGE"
10 PRINT#2,"HOURLY-MEAN EXTREME WIND SPEED U=";U;"(M/S)"
12 PRINT#2,
14 PRINT#2,"ST","R(CM)","D(DEG)"
16 CLOSE 2
20 FOR I=1 TO 30
22 DATA -17.4,-2.1,-2.6,2.1,27.5,      -10.5,2.5,-2.8,2.7,26
24 DATA -17.5,16,-3.6,3.1,26.8,      -19.2,20.6,-3.6,3.2,27
26 DATA -15,16,-3,3.2,26.2,      -14,19,-3.2,3.8,25.8
28 DATA -12.8,19,-2.5,4.3,25,      -12.6,20,-2.2,4.8,24.6
30 DATA -11.4,21.8,-2.9,4.2,24.2,      -7,19,-1.6,3.8,23.1
32 DATA -10,18,0.0,3.2,23.6,      -11,18,0.0,3.0,23.9
34 DATA -3.3,16,1.6,3.6,22,      -2.9,18.5,1.2,3.9,21.5
36 DATA -2.8,18.5,1.2,4.21.4,      -2.5,18.5,1.3,4.2,21
38 DATA -2,14.5,1.4,4.3,20.7,      -.1,12.9,1.4,4.3,20.6
40 DATA 4.8,11.8,1.7,4.4,20.3,      5.8,10.5,1.6,4.2,20.3
44 DATA 10.4,10.1,1.9,4.5,19.1,      24,10.3,2.2,4.7,17.5
46 DATA 24,9,2.2,4.5,17.6,      18.4,6.3,2.3,4.1,18
48 DATA 14.8,1.5,2.6,3.6,18.1,      8.7,-7.4,1.8,2.6,18
50 DATA 6.2,-9,2.7,2.2,17,      5,-10,1.9,1.2,18.5
52 DATA 4.2,-9.6,1.4,.5,20,      3,-9,1.8,-.6,20.6
100 READ X,Y,J,K,E
111 LET X=X*(U/10)↑2
112 LET Y=Y*(U/10)↑2
113 LET J=J*(.653*U↑2+14.37*U+12.2)*.008192
114 LET K=K*(.653*U↑2+14.37*U+12.2)*.008192
119 LET A=22
120 LET B=90-A
121 LET C=COS(B*π/180)
122 LET S=SIN(B*π/180)
123 LET M=X↑2+(J*C+K*S)↑2+2*X*C*(J*C+K*S)
124 LET N=Y↑2+(K*C-J*S)↑2+2*Y*C*(K*C-J*S)
125 LET Q=2*(X*Y+(J*C+K*S)*(K*C-J*S)+X*C*(K*C-J*S)+Y*C*(J*C+K*S))
127 LET L=0.5*(180/π*ATN(ABS(Q/(M-N))))
200 IF SGN(Q)=1 THEN 202
201 GOTO 300
202 IF SGN(M-N)=1 THEN 210
203 GOTO 250
210 IF ABS(X)<=ABS(Y) AND SGN(X)=1  AND SGN(Y)=1  THEN 400
212 IF ABS(X)<=ABS(Y) AND SGN(X)=-1 AND SGN(Y)=-1 THEN 404
214 IF ABS(X)>=ABS(Y) AND SGN(X)=-1 AND SGN(Y)=-1 THEN 404
216 IF ABS(X)>=ABS(Y) AND SGN(X)=-1 ANDSGN(Y)=1   THEN 404
218 IF ABS(X)>=ABS(Y) AND SGN(X)=1  AND SGN(Y)=1  THEN 400
220 IF ABS(X)>=ABS(Y) AND SGN(X)=1  AND SGN(Y)=-1 THEN 400
222 IF SGN(M-N)=1 THEN
224 GOTO 600
250 IF ABS(X)<=ABS(Y) AND SGN(X)=1  AND SGN(Y)=1  THEN 408
252 IF ABS(X)<=ABS(Y) AND SGN(X)=-1 AND SGN(Y)=1  THEN 408
254 IF ABS(X)<=ABS(Y) AND SGN(X)=-1 AND SGN(Y)=-1 THEN 412
256 IF ABS(X)<=ABS(Y) AND SGN(X)=1  AND SGN(Y)=-1 THEN 412
258 IF ABS(X)>=ABS(Y) AND SGN(X)=-1 AND SGN(Y)=-1 THEN 412
260 IF ABS(X)>=ABS(Y) AND SGN(X)=1  AND SGN(Y)=1  THEN 408
262 IF SGN(Q)=-1 THEN 300
264 GOTO 600
270 IF SGN(Q)=-1 THEN 300
271 GOTO 600
300 IF SGN(M-N)=-1 THEN 304
302 GOTO 318
304 IF ABS(X)<=ABS(Y) AND SGN(X)=1  AND SGN(Y)=1  THEN 416
306 IF ABS(X)<=ABS(Y) AND SGN(X)=-1 AND SGN(Y)=1  THEN 416
308 IF ABS(X)<=ABS(Y) AND SGN(X)=-1 AND SGN(Y)=-1 THEN 420
310 IF ABS(X)<=ABS(Y) AND SGN(X)=1  AND SGN(Y)=-1 THEN 420
312 IF ABS(X)>=ABS(Y) AND SGN(X)=1  AND SGN(Y)=-1 THEN 420
314 IF ABS(X)>=ABS(Y) AND SGN(X)=-1 AND SGN(Y)=1  THEN 416
318 IF SGN(M-N)=1 THEN 350
320 GOTO 600
350 IF ABS(X)<=ABS(Y) AND SGN(X)=-1 AND SGN(Y)=1  THEN 424
352 IF ABS(X)<=ABS(Y) AND SGN(X)=1  AND SGN(Y)=-1 THEN 428
354 IF ABS(X)>=ABS(Y) AND SGN(X)=1  AND SGN(Y)=1  THEN 428
356 IF ABS(X)>=ABS(Y) AND SGN(X)=1  AND SGN(Y)=-1 THEN 428
358 IF ABS(X)>=ABS(Y) AND SGN(X)=-1 AND SGN(Y)=-1 THEN 424
360 IF ABS(X)>=ABS(Y) AND SGN(X)=-1 AND SGN(Y)=1  THEN 424
362 GOTO 600
400 LET P=    ABS(L)
402 GOTO 500
404 LET P=180+ABS(L)
406 GOTO 500
408 LET P= 90-ABS(L)
410 GOTO 500
412 LET P=270-ABS(L)
414 GOTO 500
416 LET P= 90+ABS(L)
418 GOTO 500
420 LET P=270+ABS(L)
422 GOTO 500
424 LET P=180-ABS(L)
426 GOTO 500
428 LET P=360-ABS(L)
500 LET F=COS(P*π/180)
502 LET G=SIN(P*π/180)
504 LET R=SQR(M*F↑2+N*G↑2+Q*F*G)
506 LET D=P-E-90
508 IF SGN(D)=1 THEN 522
510 LET D=360+D
522 LET R=INT(R+.5)
524 LET D=INT(D+.5)
526 OPEN 3,4
528 CMD 3
530 PRINT#3,I,R,D
532 CLOSE 3
534 NEXT I
536 END
600 OPEN 3,4
602 CMD 3
604 PRINT#3, "CHECK DATA"
608 CLOSE 3
```

It is difficult to prove the predicted results of a once-in-50 year surge, unless we wait another 50 years. A method which can evaluate our predictions is to use the highest surge records in the past. However, tidal stations in the past were limited to the coast only, and not many stations along the North Sea coast have reliable continuous records for longer than say 30 years. A few particular places on the North Sea coast have historical records of abnormal high-water levels (tides plus surges without separation) for nearly 100 years, but these places are not all suitable for surge measurements, and some measurements are not made with scientific instruments. Also conditions relating to surges in the past 50 years might not be the same as for another 50 years. Comparisons of the same predictions approached by different methods will be a compromise, but an agreement of their results alone does not necessarily prove that the predictions are correct.

Bearing these facts in mind, Fig. 22 has been prepared to evaluate the predicted extreme surge shown in Fig. 21. The horizontal axis of the diagram represents the North Sea coast with names of tidal stations and approximate positions, and the vertical axis represents surge heights. The solid line shows the predicted once-in-50 year extreme surge height for the coastal line, obtained by the author's method (1976). The dotted line shows an equivalent result provisionally obtained by Flather (1980) from his dynamic method. The three circles show also equivalent surge heights at three coastal stations, obtained by Pugh and Vassie (1978) from their statistical analysis of observational surge data. A vertical bar shows the highest surge value (with the data) recorded at each station from the material available to the author. Most of his material covers a period of the past 30 years approximately, although it is not continuous.

In this comparison, if any predicted extreme value is below the recorded value, we can say that the prediction is not correct. On the other hand, a predicted value exceeding the recorded value with a large margin is not necessarily a great over-estimation. In this sense, the author's prediction is reasonable for about two thirds of the North Sea coast. Along the remaining one third of the coast from Ostend to Esbjerg, the author's predicted values are below the recorded maximum values.

The value of $\underline{S}$ (km) shown along the horizontal axis of the diagram is an approximate distance from the nearest bottom contour of 10 m. At a tidal station with a large value of $\underline{S}$, a higher local effect of surge generation is expected. For example, compare data for Cuxhaven and Büsum against Heligoland. The relatively poor results of the author's prediction for the southern North Sea coast is probably due to an imperfection in representing a very shallow-water area by his model.

There is no material to prove the prediction for the offshore area of the North Sea coast at the moment.

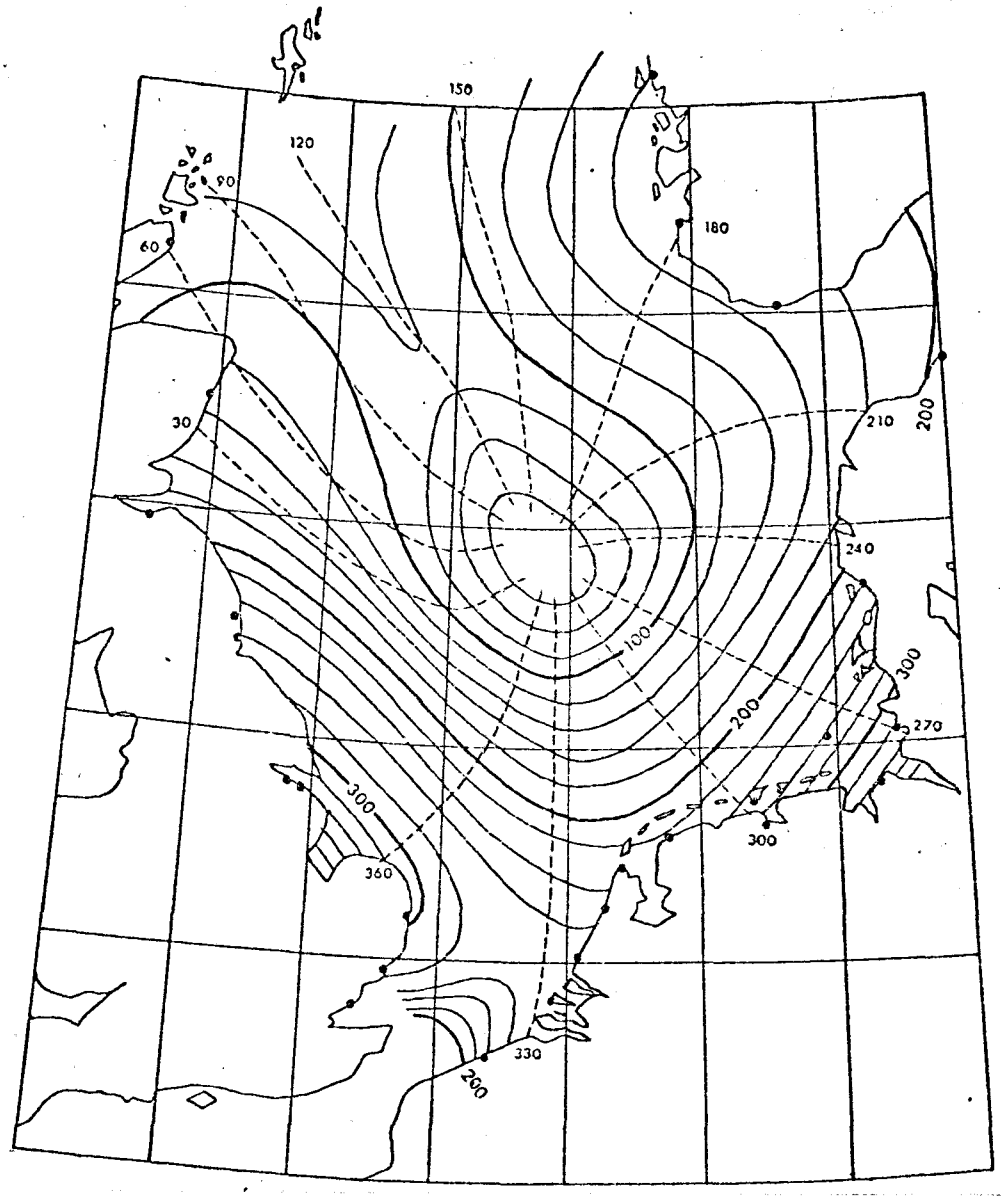

Fig. 21 Example of an extreme surge height diagram for the hourly-mean wind speed of 36 m/s, obtained by Type-B prediction procedure (Ishiguro, 1976).

Solid line: Surge height (cm). Dotted line: Wind direction (degrees) which generates the maximum surge at each point in the sea.
Example of use At a point of 54.0°N and 2.0°E, the extreme surge height is 216 cm above a predicted tidal level, and the direction of wind which generates such a surge is 3.5°.

The wind/pressure field is applied over a limited area of the North Sea (inside of the line from Wick to Bergen), i.e. external surges are not included. The diagram shows states when surges are fully developed under specific wind/pressure fields. If external surges are included, and/or in a state other than fully developed, surge heights in some areas (notably near the centre of the sea) would be greater than the values shown.

The surge height at each point is determined by the penultimate equation in Fig. 18, which is a function of wind direction, θ_w. The maximum surge height has been obtained by choosing θ_w from any value (0-360°) so that the height becomes maximum, since the combined probability of direction and speed of extreme winds is not known.

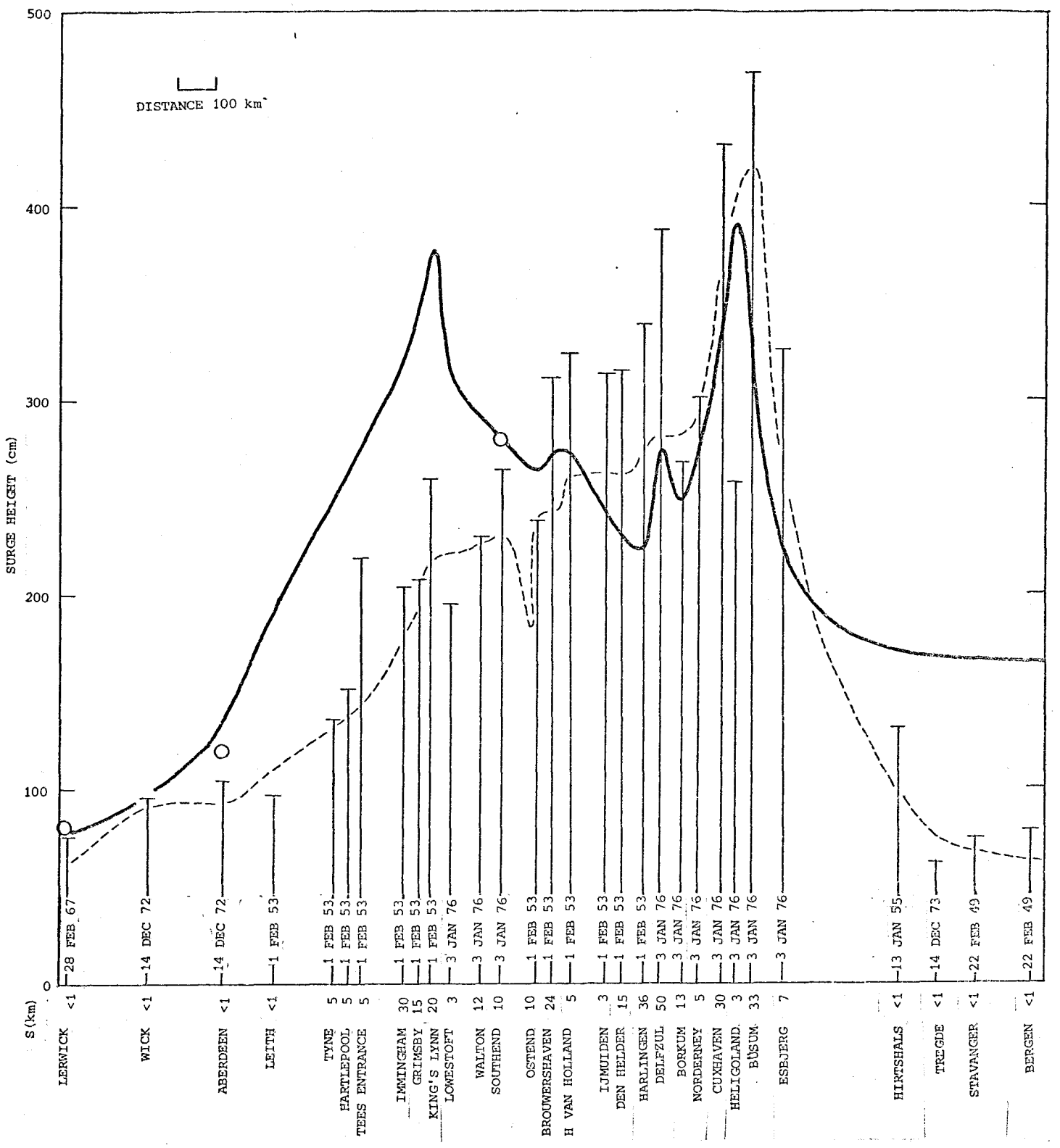

Fig. 22 Comparisons of the extreme surge heights computed by the two dynamic methods and a statistical method with the surge heights observed along the North Sea coast.

——— Extreme surge for the hourly-mean wind speed of 36 m/s over the North Sea, with the pressure field, response times, and wind-speed averaging factor, computed by Ishiguro (1976).

--- Maximum surge computed by Flather (1980).

O 50-year extreme surge height derived from the observational data, statistically computed by Pugh & Vassie (1978).

T Highest surge for each station in the observational data available to Ishiguro (1980), with the date of occurrence.

S Approximate distance (km) from a tidal station to the nearest bottom contour of 10 m (undisturbed water depth).

5. COMPARISONS OF THE METHOD WITH OTHER METHODS

The suitability of a storm surge prediction method depends on the characteristics of each sea, e.g. the dimensions of the sea area, water depth, shape and latitude. Therefore, the discussion is limited to the North Sea.

Table 3 shows the comparisons of the method (Type-A) with other daily-surge prediction methods, which are used for surge prediction services or potentially useful for them. The classification, with names, has been made only for the author's convenience, while each method has a finer variation with a name given by each worker. An empirical-formula method has been used for a storm surge warning system in Britain since 1953, and probably in some other countries around the North Sea. It is not certain, to the author, if any dynamic method is used for a routine prediction service in any country, although some trials of dynamic methods for actual services has been carried out.

The accuracy of surge height prediction by each method is one of the most important factors to compare. However, it is difficult to obtain such an exact value, because most methods are still being improved, and some values available at a certain date do not indicate the accuracies of the methods themselves. Therefore, the indication of accuracies is omitted from the table.

The accuracy of any daily-surge prediction method greatly depends on the accuracy of the weather forecast. Therefore, the accuracy of each method should be evaluated with an assumption that the weather forecast is 'perfect' which can be simulated by observed data.

Table 4 shows comparisons of the method (Type-B) with other long-term extreme surge prediction methods. The classification and the name of each method are again for the author's convenience.

The comparison of accuracy of methods is again difficult, since observational data are not available unless we wait a predicted period (e.g. 50 years).

Any long-term extreme surge prediction is related to a statistical treatment, involving a probability problem either in meteorological data or surge data, which were observed in say 50 years. The prediction is based on an assumption that the same probability of occurrences is continued from the past to the future. There are some investigations which do not support this assumption. To apply a probability theory to meteorological data, rather than surge data, has an advantage that a representative area by the former is somewhat greater than the latter. Also meteorological observations have a longer history than surge observations, and there are more long-running meteorological stations than tidal stations. On the other hand, a statistical treatment of surge data is more direct.

Table 3 Comparisons of daily-surge prediction methods

	Empirical-formula methods	Other dynamic methods	Dynamic method in this paper (Type-A)
Input required	Observed meteorological and surge data for several hours. Forecast meteorological data for a few hours or days.	Observed meteorological and surge data for several hours. Forecast meteorological data for a few hours or days.	Forecast meteorological data for several hours to a few days only.
Amount of data	Relatively small. Different formula for each point.	Large.	Very small.
Output available	Generally for a few particular coastal points. Maximum surge height and/or time-varying surge height for each point.	For the whole sea area. A continuous surge height varying with time for each point.	For the whole sea area. Maximum surge height and approximate duration for each point.
Scale of input-data transmission	Medium.	Large.	Very small (e.g. telephone).
Scale of computer	Small.	Large.	Small.
Running cost	Small.	Considerable.	Small.

The accuracy of any method greatly depends on that of the meteorological forecast. Providing the meteorological forecast is perfect, the accuracy of predicted surge heights is potentially the best for 'other dynamic methods', in principle, since these methods have less simplification than the rest of the methods. If the meteorological forecasts with their present accuracy are used, and if each surge prediction method is well developed, the accuracy of predicted surge heights will be of the same order throughout all the method.

Table 4 Comparisons of long-term extreme surge prediction methods

	Statistical method	Displaced dynamic method	Dynamic-statistical method	Dynamic method in this paper (Type-B)
Input required	Observed surge data at each station for many years.	Observed wind/pressure data over the whole sea for a few extreme surge cases.	Observed wind/pressure data over the whole sea surface for many surge cases.	Extreme wind speed over the sea surface only.
Output available	Extreme surge height around the above station only.	Extreme surge height in a relatively small area of the sea.	Extreme surge heights in the whole sea area.	Extreme surge heights in the whole sea area. Direction and duration of wind, at each point, which generate the extreme surge.
Operation	Statistical treatment of the input data.	Dynamic simulations of a few surge cases with the input data, but with displaced positions so that surge heights become maximum in the small area.	After each surge case is dynamically simulated, surge heights at each point are analysed.	As explained in section 4.2 of this paper.

It is not possible to compare a predicted value with a real value, unless we wait the prediction period (e.g. 50 years). Therefore, the accuracy of each method is not known. No method can predict the date when the extreme surge will occur. The time and cost for obtaining a prediction is not critical, since the prediction does not have to be repeated.

6. FURTHER IMPROVEMENTS OF THE METHOD

The method is still being improved, especially in the following directions:

1 Improvements of a dynamic model of the sea from which the values of X, Y, J, K (see pages 19 and 31) for the method are derived;

2 Improvements of the sampling technique of the input data (wind direction etc.) for Type-A prediction, including the treatment of weather forecast data;

3 Improvements of statistical treatment of the input data for Type-B prediction, and

4 Determination of a wind/pressure field area which makes a surge height maximum at a point for Type-B prediction.

Some details of these subjects are explained in this chapter.

6.1 Dynamic model

In principle, most dynamic models (numerical or electronic) can be used for obtaining the values of X, Y, J, K on which the method is based. Obviously, the accuracy of a dynamic model greatly affects results obtained by the method.

For the examples shown in this paper, the values of X, Y, J, K have been derived from the author's earlier electronic model of the North Sea, which has mixed grid sizes of 50 and 100 km squares, and the northern boundary to the open sea on the line connecting Wick to Bergen (not along the continental shelf).

Model grids having large dimensions make the resolution of surge heights critical in an area of the sea where the coastal line is complex, although this is less critical in offshore areas. A solution for this problem is to use smaller grids, as in the new electronic model.

The representation of surges by conventional types of grids becomes critical for a very shallow water area, which often coincides with an area having a complex coastal line, e.g. the difficulty of accurate surge predictions for Cuxhaven and Busum (see Fig. 14 and Fig. 22). A solution is to use a different type of grid, in a combination of a conventional type, for shallow water areas.

The missing area from the model most seriously affects 'external surges' which are known to be generated mainly along the north-west coast of Scotland. A simple solution is to extend the model area, and this has already been done for the new electronic model. A temporary solution applied to Type-A prediction in this paper is to correct the values of X (preferably J too), by using information of external surge propagation in the North Sea. Predictions to which this correction are applied are indicated by X+C (see Fig. 13 and 14). See Appendix 3 for the details of the correction.

Treatment of external surges for Type-B prediction is not the same as for Type-A prediction, and this is explained in Section 6.4.

6.2 Sampling of input data

For the input data of the method (Type-A), a wind speed, wind direction and duration, have to be sampled from a set of forecast wind/pressure field data. Apart from the accuracy of the forecast data, an appropriate sampling of the input data improves the accuracy of the surge prediction.

The author is particularly interested in improving the input sampling technique which is closely related to weather forecast practice. The technique must take into account the position of a storm system relative to the sea, as shown in Fig. 7.

6.3 Statistical treatment of data

For a long-term extreme surge prediction, a statistical treatment of data cannot be avoided, either for the input or output data of the prediction. The method uses, at the moment, statistically treated wind speed data by Shellard as the input data, without other information. Consequently, the wind direction has to be chosen in such a way that it makes the surge height at a point maximum when this is combined with other factors. In practice, our experience (though less than 50 years) tells that most great surges in the North Sea occurred with wind directions within a certain limited range. If we know the probability of an extreme wind in combination with its speed and direction, an extreme surge prediction (as shown in Fig. 21) would become more realistic. On the other hand, we should be aware of the danger of assuming such a condition without sufficient evidence.

Whether a probability derived from the observed data for a certain period can be extended toward the future is another important problem.

6.4 Determination of a field area

Unlike Type-A prediction, for which a size of wind/pressure field is known from a weather forecast, in principle, it is difficult to know the size of such a field for a long-term surge prediction (Type-B). It is important that the largest field does not necessarily generate a maximum surge height at any point in the sea area. Therefore we have to determine the relationship between the size of a field and the surge height at a point in question, as well as the effect of a combination of more than one field each of which has a different size, direction and intensity.

A predicted result obtained from a model which does not fully cover the North Sea (like Fig. 21) contains this problem; i.e. the low-surge area in the centre of the sea in this figure is formed only when the field is limited to the main part of the North Sea.

The author is planning to solve this problem by treating each sea area separately first, then making combinations of the results in order to produce the maximum surge at each point.

7. CONCLUSIONS

A practical storm-surge prediction method has been developed with two variations. Type-A is for daily surge predictions which require only three parameters to be specified by each user. Type-B is for extreme-surge predictions which require only one parameter to be specified. The whole programme and constant data for a particular sea (the North Sea in this example) are written in a basic language and recorded on a cassette tape, so that most users can operate it with a small table-top computer. By specifying the parameters, the maximum surge height at each of 30 coastal and 60 offshore stations can be obtained immediately. The values of the parameters (a wind speed, direction and duration in a certain state) for Type-A prediction can be obtained from a weather forecast, and the values can be communicated even by telephone.

The results obtained from the method have been compared with surge data observed along the North Sea coast, and show its usefulness. Improvements are being carried out, especially to extend the sea area (i.e. to include external surges).

ACKNOWLEDGEMENTS

Observed data of 17 surge cases in the North Sea, only two of which are shown in this paper, have been used in this investigation. They include data specially supplied from the authorities in the Netherlands, Germany, Denmark and Norway, through the UK Marine Information Service. The author is grateful for their kind cooperation.

The author is also grateful to Miss Kathleen Reeves-Wilkin for her assistance in various ways in this project.

REFERENCES

(1) Dietrich, G. et al. (1952)
Wind conditions over the sea around Britain during 1900-1946, The German Hydrographic Institute, Hamburg, pp. 38.

(2) Dolata, F. & Engel, M. (1979)
Sturmflutvorhersagen mit mathematische-physikalischen modellen, Die Küste, 34, pp. 203-255.

(3) Duun-Christensen, J.T. (1975)
The representation of the surface pressure field in two-dimensional hydrodynamic numeric model for the North Sea, the Skagerrak and the Kattegat,
DHZ, 28, pp. 97-116.

(4) Flather, R.A. (1980)
Maximum tidal and storm surge current over the continental shelf - preliminary results from a numerical model,
IOS Internal Document, 103, pp. 15.

(5) Harding, J. & Binding, A.A. (1978)
Wind field during gales in the North Sea and the gales of 3 January 1976,
Meteorological Magazine, 107 , pp. 164-181.

(6) Hasse, L. (1974)
On the surface to geostrophic wind relationship at the stability dependence of the resistance law,
Beiträge zur Physik der Atmosphäre, 47, pp. 45-55.

(7) Heaps, N. (1969)
A two-dimensional numerical sea model.
Phil. Trans. Royal Soc. London, A-265, pp. 93-137.

(8) Ishiguro, S. (1964)
Detailed structure of a storm surge in the North Sea,
Revue Pétrolière, 1073, Section I, No. 110, pp. 1-5.

(9) Ishiguro, S. (1966)
Storm surge in the North Sea,
Advisory Committee on Oceanographic & Meteorological Research,
Paper 25(iii), pp. 1-57.

(10) Ishiguro, S. (1972)
An electronic model for tides and storm surges in the North Sea,
IOS Internal Report, , pp. 1-234.

(11) Ishiguro, S. (1976)
Highest surge in the North Sea,
IOS Internal Report, 36, pp. 1-31.

(12) Ishiguro, S. (1976)
Pressure-generated surge in the North Sea.
IOS Internal Report, 35, pp. 1-26.

(13) Ishiguro, S. (1980)
Water-level response to a semi-diurnal sinusoidal wave
excitation in the North Sea.
IOS Internal Document, 99, pp. 1-21.

(14) Ishiguro, S. (1980)
Position of the minimum-surge area in the North Sea relating
to quasi uniform steady wind/pressure fields,
IOS Internal Document, 100, pp. 1-13.

(15) Ishiguro, S. (1980)
Formulation of the speed-averaging factor for once-in-50 year
extreme wind in storm surge prediction,
IOS Internal Document, 117, pp. 1-5.

(16) Netherlands Delta Committee (1960)
Meteorological and oceanographical aspects of storm surges
on the Netherlands coast, pp. 96.

(17) Pugh, D.T. & Vassie, J.M. (1978)
Extreme sea levels from tide and surge probability,
Proc. 16th Coastal Engineering Conference, Hamburg,
1, pp. 911-930.

(18) Shellard, H.C. (1975)
Lerwick anemograph records 1957-70 and the offshore industry,
Meteorological Magazine, 104, pp. 189-208.

(19) Shellard, H.C. (1977)
Hourly-mean wind speed above the sea surface with an average
recurrence period of 50 years,
Offshore installations: Guidance on design and construction,
2, pp. 20.

APPENDIX 1 ABBREVIATIONS AND POSITIONS OF COASTAL STATIONS

WK	Wick	58 26N	3 05W
AB	Aberdeen	57 09N	2 05W
DD	Dundee	56 27N	2 58W
LE	Leith	55 59N	3 10W
DB	Dunbar	56 00N	2 31W
BW	Berwick	55 47N	2 00W
TY	Tynemouth	55 01N	1 24W
HP	Harlepool	54 41N	1 11W
TE	Tees	54 38N	1 09W
HU	Hull	53 45N	0 19W
IM	Immingham	53 37N	0 11W
GM	Grimsby	53 35N	0 04W
KL	King's Lynn	54 45N	0 24E
LT	Lowestoft	52 28N	1 45E
HS	Holland Sluice	51 49N	1 14E
SE	Southend	51 31N	0 35E
DV	Dover	51 07N	1 19E
OE	Ostend	51 14N	2 55E
VL	Vlissingen	51 27N	3 36E
BH	Brouwershaven	51 44N	3 55E
HH	Hook van Holland	51 59N	4 07E
IJ	Ijmuiden	52 28N	3 34E
DH	Den Helder	52 58N	4 45E
TL	West Terschelling	53 22N	5 13E
DF	Delfzjl	52 28N	4 34E
HL	Harlingen	53 10N	5 25E
BK	Borkum	53 35N	6 39E
ND	Norderney	53 42N	7 10E
CX	Cuxhaven	53 52N	8 43E
BU	Büsum	54 08N	8 51E
LS	List	55 01N	8 27E
EJ	Esbjerg	55 28N	8 27E
TH	Thybøron	56 42N	8 13E
HI	Hirtshals	57 36N	9 57E
TG	Tregde	58.00N	7 34E
SV	Stavanger	58 58N	5 44E
BG	Bergen	61 56N	5 07E

APPENDIX 2 WIND-PRESSURE CONVERSION

Both Type-A and Type-B prediction procedures require a wind-to-pressure conversion. In either case, this could be a pressure-to-wind conversion, if the predicted pressure data is available first. Three different formulas have been used by the author:

(1) $\frac{\partial p}{\partial l} = 0.222U$ $\qquad \alpha = 12^{\circ}$

This was based on Dietrich et al. (1952), and had been used by the author for this method from 1966 to 1975.

(2) $\frac{\partial p}{\partial l} = (U - 2.4)/4.68$ $\qquad \alpha = 22^{\circ}$

This is based on Hasse (1974), with chosen values by the author, and used for this method from 1976 to 1979.

(3) $\frac{\partial p}{\partial l} = (0.653U^2 + 14.37U + 12.20) \times 0.8192 \times 10^{-2}$ $\qquad \alpha = 22^{\circ}$

This is based on Hasse (1974), improved by Duun-Christensen (1976), modified by the author with the chosen values and is now used for this application. 0.8192 is derived from a fixed latitude of 55°N.

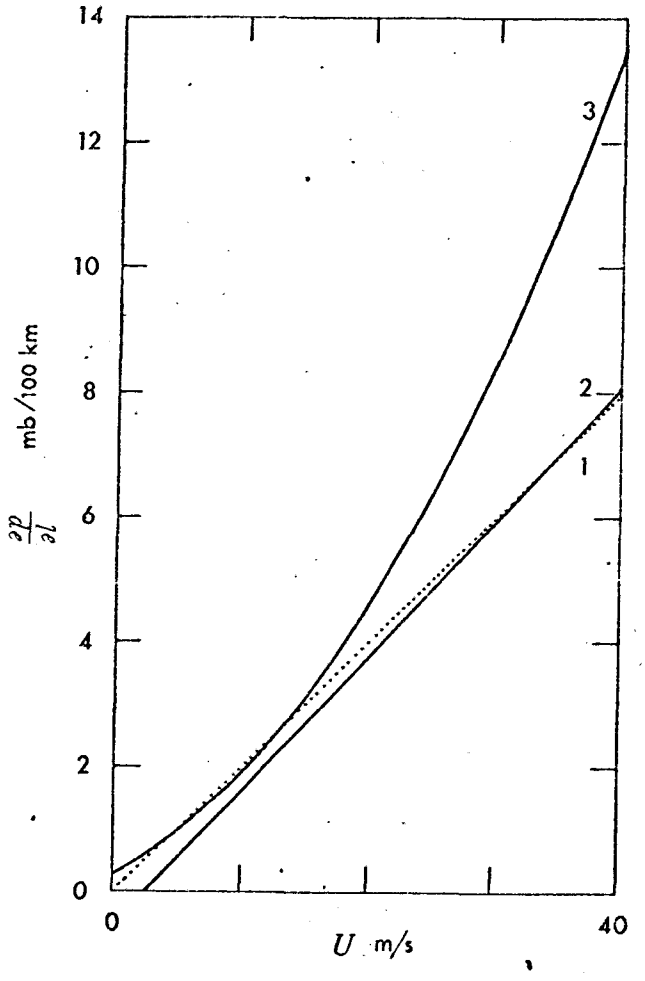

Throughout the three formulae,

U : Wind speed
m/s

$\frac{\partial p}{\partial l}$: Pressure gradient
mb/100 km

α : Angle between wind direction and an isobar
degrees

APPENDIX 3 CORRECTION FOR EXTERNAL SURGES

The author's earlier electronic model of the North Sea is terminated at a line from Wick to Bergen (instead of along the continental shelf). This has an effect on the value of X, Y, J, K for the method, as described in section 6.4. The effect is considered to be most serious for X, next for J, and has only a minor effect on Y and K. A temporary correction of the effect on X, which is indicated by X+C in Figs. 13 and 14, is described here.

The correction is based on the idea that certain values representing a 'typical' external surge be added to values of X. The typical surges are selected from the author's investigation of the characteristics of propagation of external surges in the North Sea (Ishiguro, 1966).

According to this material, the pattern of an external surge entered into the North Sea is mainly determined by the position of entrance, an average height and duration (pulse width) measured at the entrance (the northern entrance of the North Sea), and relatively little affected by detailed variations in its shape (in space and time).

Fig. A1 shows propagation characteristics of an external surge with an artificial pattern, computed by Ishiguro (1966). The height reduces exponentially along the line from Wick to Bergen, and also varies with time in gaussian shape. Fig. A2 shows a simulated external surge under observed meteorological conditions, computed by Heaps (1969). The propagation characteristics shown in the two diagrams are essentially the same.

Fig. A3 is an extract of the analysis (Ishiguro, 1966) of an external surge in the North Sea. In this analysis, the external surge is represented by a step function (front length 100 km, height 100%) and injected continuously into the sea through a line near the Orkney Islands, then the water-level contours at various times (2 to 40 hours) are obtained.

Gathering this type of information, which is represented by Figs. A1, A2 and A3, the following procedure of correction of values of X has been decided.

One of the diagrams in Fig. A3 (the full version of the set has finer intervals), which has the same duration (pulse width) as the duration of a sampled wind/pressure field for the factor X, is selected first. A contour value (%) in the selected diagram for each point of X is read next. Then 40 cm, which is assumed to be the typical initial surge height, is multiplied by the read value in %, so that an external surge height at the point and at the specific time is obtained.

After the values of X, Y, J, K from the new electronic model have been introduced to the prediction method, this temporary correction procedure will not be used.

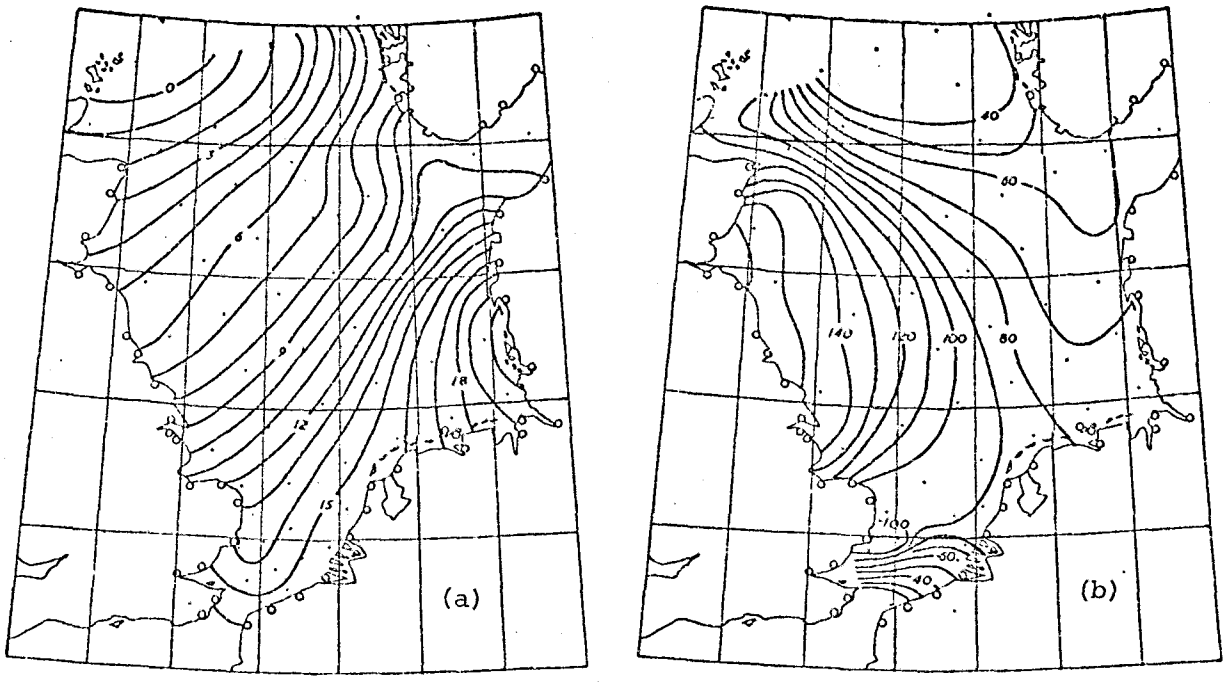

Fig. A1 Propagation characteristics of an external surge in the North Sea, computed by Ishiguro (1966).
(a) Propagation time of the maxima, hours.
(b) Ratio of the maximum surge height to the initial height, (%).

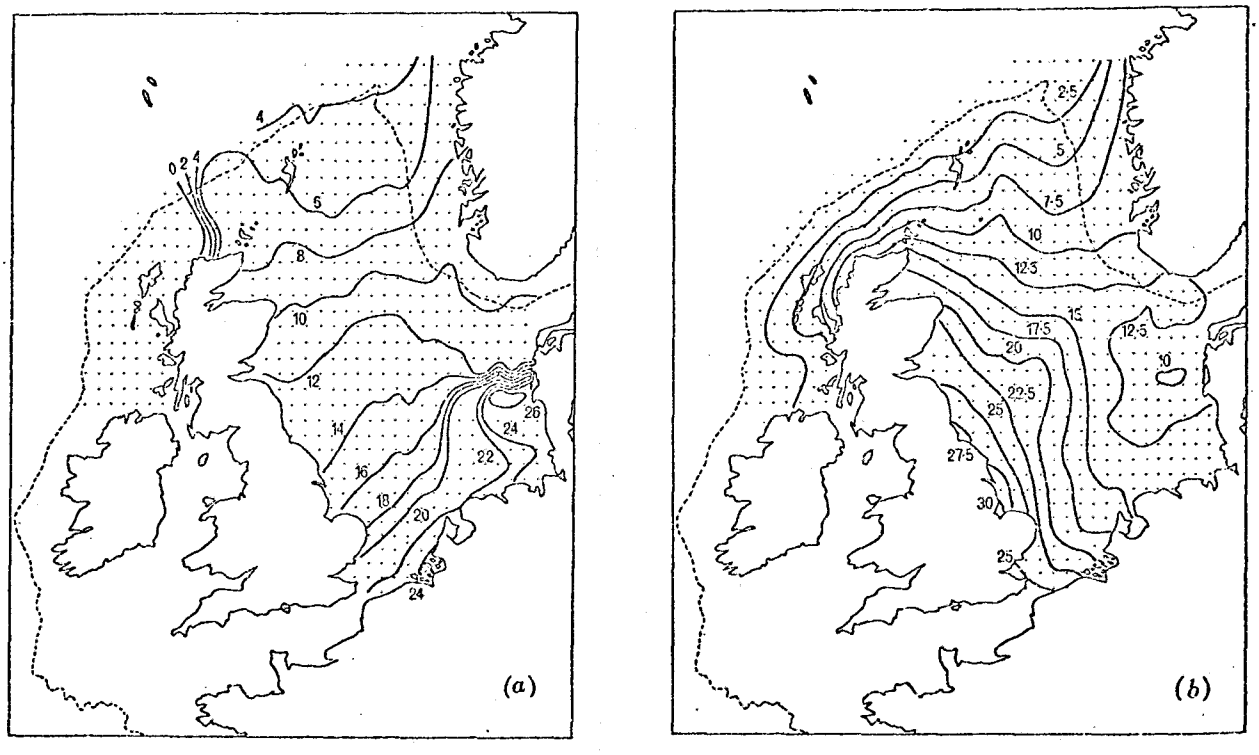

Fig. A2 Propagation characteristics of a simulated external surge from the wind/pressure field of 13 to 15 September 1956, by Heaps (1969).
(a) Propagation time of the maxima, hours.
(b) Contours of maximum elevation (in unit of 0.1 ft).

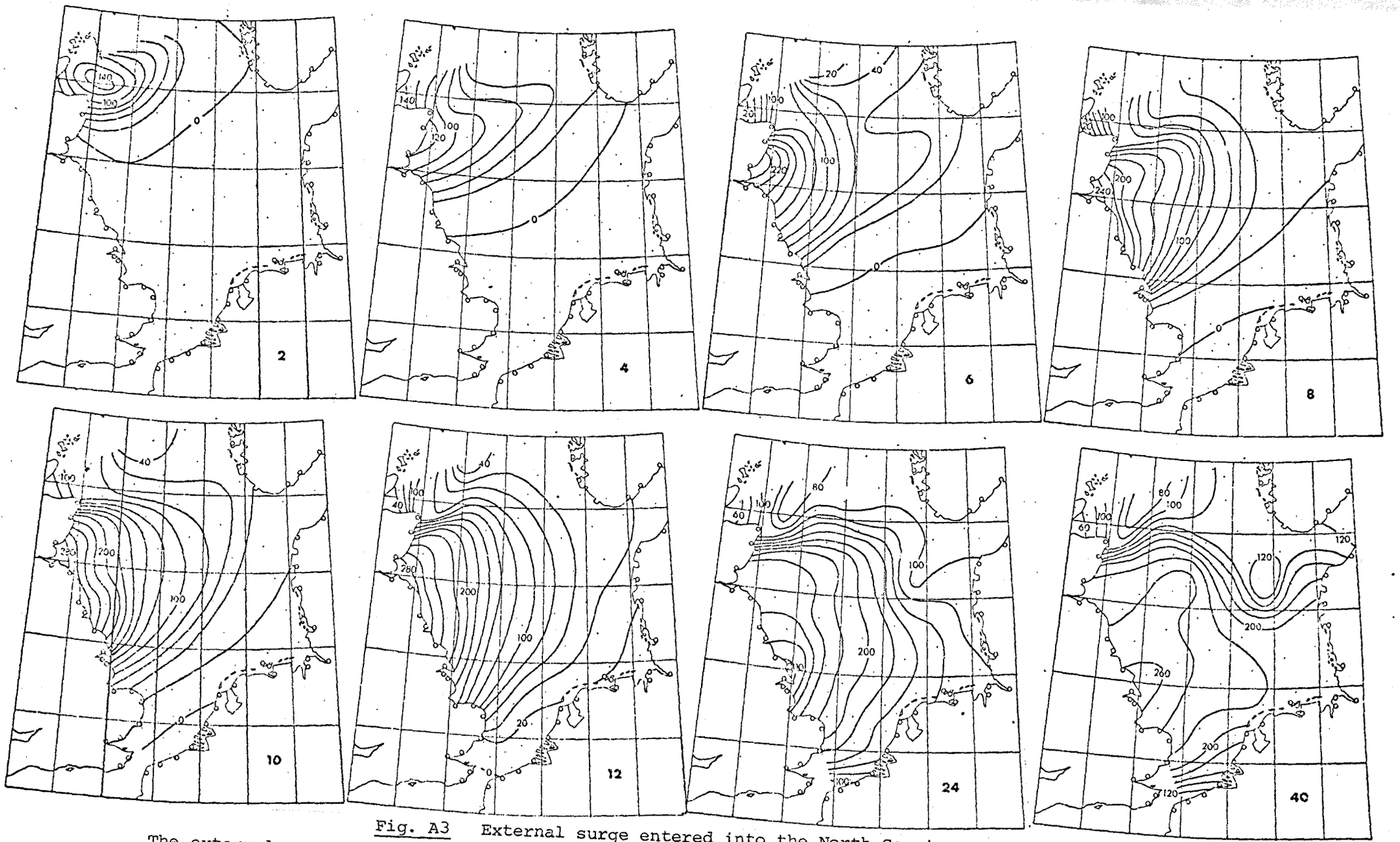

Fig. A3 External surge entered into the North Sea in a calm state.
The external surge is represented by a step function (front length 100 km, height 100%), and injected continuously into the sea through a line near the Orkney Islands , then the water level contours at various times (2 to 40 hours) are obtained. Computed by Ishiguro (1966).